Inorganic Chemistry Laboratory

Department of Chemistry

University of Oxford

Preparation of bulk and supported Co/Mo carbide catalysts for CO_2 conversion

A Thesis Submitted for the Degree of

Master of Science (by research), 2013

Naif Almuqati

St.Catherine's College, Oxford




بسم الله الرحمن الرحيم

DEDICATION

In the name of Allah, most merciful, most gracious

I would like to dedicate this work to;

My father, keeper's god, who was the first to encourage and support me in my life.
My dear beloved mother, may Allah preserve her, who was praying to Allah for me every day.

All my brothers and sisters, who have always encouraged and supported me for my further study.

Lastly to all my friends in Saudi Arabia, Kuwait and the UK, who have always encouraged and supported me throughout my study.

ACKNOWLEDGEMENTS

All the praise goes to Allah for his generous blessings, without which I would not have completed this work.

My utmost deep and sincere gratitude to Prof. Peter P. Edwards, my supervisor, teacher and friend. I have learnt a lot from you, from your intelligence, creativity, patience and attention to detail. Thanks for your invaluable support and encouragement since day one in Oxford. I am grateful to have been part of your group, working amongst dedicated scientists, in an excellent scientific environment of learning and exchange. I thank you for the confidence that you have in me and in the work that I do. Thank you very much Prof. Edwards your pre-eminent supervision.

I would also like to express my gratitude and thanks to Dr. Hamid Almegren the director of petrochemical institute at KACST, who generously gave me this chance to complete my studies.

I would like to thank Dr. Tiancun Xiao for his support, helpful discussions and for his encouragement during my study.

I am very grateful to Dr. Vladimir Kuznetsov and Dr. Liam France for their help, support and ideas over the last year. Without them, this project would have been much more difficult.

To my co-workers, Xian Du and Christopher Greenwood, thank you for helping me along during our work in this project.

Thanks to all the member of the Edwards group and specifically to the KOPRC group for many interesting discussions.

I would also like to thank Afrah Aldawsari and Nazanin Rashidi for help me when I needed to use the powder X-ray Diffraction.

Family and Friends, simply saying “thank you” does not even begin to express my heartfelt gratitude to you all.

Naif, Oxford

SUMMARY

This thesis investigates the preparation and characterisation of Co/Mo bimetallic carbides and their stability and catalytic activity as bulk catalysts for the Dry Methane Reforming (DMR) reaction and as supported catalysts on alumina. The DMR reaction was chosen due to its importance in producing syngas, as a precursor for liquid fuels, from CO_2 and CH_4, two greenhouse gases.

Bulk and supported bimetallic carbides were prepared by reductive carburization of the oxides with various hydrocarbons. The resultant carbides were characterized by X-Ray diffraction.

Reactivity studies were undertaken by investigating the variable temperature reactivity of the catalysts on the DMR reaction.

Characterization studies indicate that the oxides were transformed to the carbides successfully and these carbides had significant catalytic activity and were stable under the conditions used in the investigations.

Table of Contents

Dedication ..... **III**

Acknowledgements ..... **IV**

Summary ..... **VI**

Table of contents ..... **VII**

List of tables ..... **IX**

List of figures ..... **X**

Abbreviations ..... **XII**

Chapter One: Introduction ***1***

1.1 Background 1

1.2 Synthesis gas production and metal carbide processes 2

1.2.1 Partial oxidation of methane (POM) 2

1.2.2 Steam reforming (SR) 2

1.2.3 Dry methane reforming (DMR) 3

1.3 Selection of metal catalysts 4

1.4 Catalyst supports 5

1.5 Bimetallic carbide catalysts 5

1.6 Supported metal carbide catalysts 6

1.7 Synthesis and characterisation of catalysts and their precursors 7

1.8 Catalytic activity 9

1.9 Aim of the project 9

Chapter Two: Experimental Methods ***10***

2.1 Chemicals 10

2.2 Preparation of Co/Mo Catalyst 11

2.2.1 Preparation of $Co_{0.4}Mo_{0.6}O_x$ 11

2.2.2 Preparation of $CoMoPO_x$ 12
2.2.3 Conversion from $Co_{0.4}Mo_{0.6}O_x$ to $Co_{0.4}Mo_{0.6}C_x$ 12
2.3 X-ray powder diffraction (XRD) analysis 13
2.4 Gas chromatography (GC) analysis 14
2.5 Catalyst testing 17
2.5.1 Variable temperature testing 17
2.5.2 Catalyst stability studies 19
Chapter Three: Results and discussion ***21***
3.1 Characterisation of materials 21
3.1.1 Oxides 21
3.1.2 Carbide 26
3.2 Catalytic test 28
3.3 Stability of catalysts with temperature 29
3.3.1 Stability of bulk catalyst 29
3.3.2 Stability of the supported catalysts 33
3.3.3 Catalyst stability tests 37
3.3.3.1 Stability of catalysts with time 37
3.3.3.2 Stability tests of supported catalysts 40
3.4 X-ray analysis of catalysts pre and post-reactions 44
3.5 Discussion 47
3.5.1 Bulk catalysts (no support) 48
3.5.2 Supported catalysts 50
Chapter Four: Conclusions ***51***
4 Conclusions 51
References ***53***

List of Tables

Table 1: Comparison of characteristics of GC detectors [49, 50] 16

Table 2: Summary of the results of the effectiveness of the catalysts 47

List of Figures

Figure 1: The crystal structure of Mo_2C [43] 8

Figure 2: The crystal structure of $CoMoO_4$ [45, 46] 8

Figure 3: The tube furnace used for conversion of Co/Mo oxides to the corresponding carbides, showing the quartz tube inside the furnace connected to supplies of CH_4 and H_2 13

Figure 4: PW3040/60 X'pert PRO Console diffractometer 14

Figure 5: Shimadzu GC-2014 17

Figure 6: The bench top MicroReactor 10A 18

Figure 6-1: Schematic of the MicroReactor used in the catalyst evaluation in this work 18

Figure 7: A typical variable temperature setting for the catalyst test 20

Figure 8: A typical catalyst stability test of the reactor condition setting 20

Figure 9: Variable temperature X-ray powder diffraction patterns of $(NH_4)_6Mo_7O_{24}{\cdot}4H_2O$ 22

Figure 10: X-ray powder diffraction pattern of MoO_3 bulk material synthesised by heating ammonium heptamolybdate at 600°C 22

Figure 11: X-ray analysis of (a) MoO_3 bulk [present study] and (b) from Leisegang *et.al.* [55] 23

Figure 12: X-ray powder diffraction pattern of Co_3O_4 bulk sample after calcination of $CoCO_3$, at 600°C for 10 hours 24

Figure 13: X-ray pattern for the Co_3O_4 bulk from Will *et. al.* [58] 24

Figure 14: X-ray powder diffraction pattern of $Co_{0.4}Mo_{0.6}O_x/\gamma\text{-}Al_2O_3$ after mixing $CoCO_3$, $(NH_4)_6Mo_7O_{24.}(H_2O)_4$ with $\gamma\text{-}Al_2O_3$ and followed by calcination at 600°C for 10 hours. $\gamma\text{-}Al_2O_3$ support peaks are represented as asterisks 25

Figure 15: X-ray powder diffraction spectra of $\gamma\text{-}Al_2O_3$ and $(Al_2O_3)_{0.9}(Mo_{1-x}Co_xO_z)_{0.1}$ bimetallic supported oxides with x = 0.2, 0.4, 0.6 and 0.8. The broad peak between 20° and 30° arises from the Co/Mo oxide phase 26

Figure 16: X-ray powder diffraction patterns of Mo_2C bulk sample after conversion from MoO_3 26

Figure 17: The X-ray analysis pattern a) of Mo_2C bulk [present study] and b) from Page *et. al.* [43] 27

Figure 18: X-ray powder diffraction pattern of $Co_{0.4}Mo_{0.6}C_x/\gamma\text{-}Al_2O_3$ 27

Figure 19: X-ray powder diffraction pattern of $CoMoPC_x$ 28

Figure 20: CH_4 conversion during the variable temperature studies of bulk mono and bimetallic carbides and one supported catalyst 29

Figure 21: CO_2 conversion during the variable temperature studies of bulk carbides and one supported catalyst..... 30

Figure 22: Dependence of the reaction product ratio (H_2/CO) over reactions time for bulk carbides and one supported catalyst 32

Figure 23: CH_4 conversion during the variable temperature studies of γ-Al_2O_3 (Alfa-Aesar) and γ-Al_2O_3-supported carbides 34

Figure 24: CO_2 conversion during the variable temperature studies of γ-Al_2O_3 (Alfa-Aesar) and γ-Al_2O_3-supported carbides 35

Figure 25: Dependence of the reaction product ratio (H_2/CO) on reactions time for supported carbides..... 36

Figure 26: CH_4 conversion during the stability studies of bulk carbides and one supported catalyst at 850°C..... 38

Figure 27: CO_2 conversion during the stability studies of bulk carbides and one supported catalyst at 850°C 39

Figure 28: Dependence of the reaction product ratio (H_2/CO) on reactions time for bulk carbides and one supported catalyst at 850°C 40

Figure 29: CH_4 conversion during the stability studies of γ-Al_2O_3-supported carbides at 850°C 41

Figure 30: CO_2 conversion during the stability studies of γ-Al_2O_3 (Alfa-Aesar) and γ-Al_2O_3 supported carbides at 850°C..... 42

Figure 31: Dependence of the reaction product ratio (H_2/CO) on reactions time for supported carbides at 850°C..... 43

Figure 32: X-ray patterns comparison of CoMoPCx before and after the catalytic test at 850°C for 300 min 44

Figure 33: X-ray patterns comparison of both the pre and post-reactions for Mo_2C bulk at 850°C for 300 min 45

Figure 34: X-ray patterns comparison of both the pre and post-reactions for $Co_{0.4}Mo_{0.6}C_x/Al_2O_3$..... 45

Figure 35: X-ray patterns comparison of both the pre and post-reactions for Mo_2C supplied by Sigma-Aldrich 46

Abbreviations

Abbreviations	Full name
SMR	Steam Methane Reforming
DMR	Dry Methane Reforming
POM	Partial Oxidation of Methane
HDN	Hydrodenitrogenation
RWGS	Reverse Water-Gas Shift
XRD	X-Ray Diffraction
GC	Gas Chromatography
TCD	Thermal Conductivity Detector
FID	Flame Ionisation Detector
Wt. %	Weight Percentage

Chapter One: Introduction

1.1 Background

The use of fossil fuels has become an integral part of modern everyday life. Their diverse uses, amongst many, include transportation fuels and energy production. As a result of its constant and diverse usage, oil has become the single most powerful driver of the world's economy [1]. The main uses of oil include the synthesis of fuels for transportation, electricity generation and the synthesis of organic materials [2, 3].

The soaring use of oil has led to global warming effects, mainly due to the production of the two most important greenhouse gases; CH_4 and CO_2 [4]. To achieve global CO_2 reduction, significant research efforts have focused on the removal of CO_2 from the air to produce useful products that may be used elsewhere [5-7]. Due to the relatively inert nature and stability of CO_2 there is an urgent need to develop a catalyst that can aid enhancing the reactivity of CO_2 in particular and develop catalysts to make useful products [5, 7]. Various studies have generated an array of useful catalysts that are successful in carrying out such transformations [5, 8]. One type of catalyst which has shown significant promise is transition metal carbides. Carbides have shown catalytic activity similar to those of noble metals [9]. Recently, molybdenum carbide has been the subject of much research interest due to its successful involvement in a large number of reactions, such as: the partial oxidation of methane (POM) [10], the steam methane reforming (SMR) [11], dry the methane reforming (DMR) [11] and the hydrodenitrogenation (HDN) reactions [12].

Recent research has highlighted that the addition of a different metal to form mixed metal carbide can significantly enhance the reactivity of molybdenum carbides [13]. To further increase the catalytic reaction processes other parameters can be employed, such as increasing the surface area by employing support materials for the catalysts. One such process is the dispersion of the catalyst onto an solid support to increase the surface area and hence enhance the reactivity of the catalyst [14]. Although the major thrust of these studies seems to be geared towards unsupported bimetallic carbides, there are a number of research areas where so-called "supported" metal carbides are of growing importance [11].

1.2 Synthesis gas production and metal carbides processes

The literature abounds with reports of a number of processes that are utilising CO_2 and/or CH_4 in reactions that produce synthesis gas (a mixture of CO and H_2) for use as a raw material in the production of liquid fuels [15]. These processes include the partial oxidation of methane (POM) [10], steam methane reforming (SMR) [11], and dry methane reforming (DMR) [11]. We discuss these reactions below.

1.2.1 Partial oxidation of methane (POM)

A useful method of producing the impotent "syngas" is the partial oxidation of methane [10] which is shown in the equation below:

$$2CH_4 + O_2 \leftrightarrows 2CO + 4H_2 \qquad \Delta H°_{298} = -35.6 \text{ kJ mol}^{-1} \qquad (1.1)$$

This process is mildly exothermic and produces a molar ratio of H_2/CO equal to 2, which makes it ideal for the Fischer-Tropsch synthesis [16] shown below:

$$(2n+1)H_2 + nCO \rightarrow C_nH_{(2n+2)} + nH_2O \qquad (1.2)$$

Catalysts employed for the POM reactions are varied and range from supported Ni, Fe or Co metals, noble metals or transition metal carbides [16]. The major problem associated this reaction is the deposition of carbon created by the decomposition of methane and the so-called Boudouard reaction to yield and C: [17]

The POM reaction is exothermic and the heat generated may be used to enhance other reactions such as SMR or DMR. Another area of utilising the heat generated is to use it to enhance other reactions, for example [17]:

$$5CH_4 + CO_2 + 2O_2 \rightleftarrows 6CO + 10H_2 \qquad \Delta H°_{298} = +104.6 \text{ kJ mol}^{-1} \qquad (1.3)$$

1.2.2 Steam reforming (SR)

Presently, the largest amount of syngas is produced by the reaction of the steam reforming of methane [11]:

$$CH_4 + H_2O \leftrightarrows CO + 3H_2 \qquad \Delta H°_{298} = +206 \text{ kJ mol}^{-1} \qquad (1.4)$$

The high endothermic nature of the reaction necessitates the use of high temperatures and catalysts [16, 18]. Currently, the most favoured industrial method is the use of nickel-based catalysts, at temperatures between 970-1100 K and pressures in excess of 3.5MPa [19]. The most accepted mechanism for this reaction involves the dissociative adsorption of methane onto the catalyst surface. This reaction, however, has its limitations; this being the relative high endothermic nature of the reaction which necessitates a high reaction temperature and thus high fuel costs. Nickel catalysts are also known to promote the formation of coke, which leads to deactivation of the catalysts. Finally, the high H_2/CO molar ratio is undesirable since this forces a further process to be undertaken to make the ratio such that liquid fuels can be synthesised [16, 18, 19, 20].

1.2.3 Dry methane reforming (DMR)

Both CH_4 and CO_2 are known greenhouse gases and there is much interest to limit their release into the atmosphere and/or to remove them from the atmosphere. A reaction, therefore, that utilises both of these gases to produce less polluting products is desirable. One such reaction is the Dry Methane Reforming Reaction (DMR) as shown below: [11]

$$CH_4 + CO_2 \leftrightarrows 2CO + 2H_2 \qquad \Delta H°_{298} = +247 \text{ kJ mol}^{-1} \qquad (1.5)$$

The (standard) enthalpy of reaction ($\Delta H°_{298}$) is also indicated. The high stability of the CO_2 molecule means that to enhance its chemical reactivity, an energy-intensive process will be required. This results in incurring high costs in converting CH_4 to liquid fuels by means of this reaction. Despite the high endothermic nature of the reaction, it can become attractive in areas where water is in short supply and SMR is not possible. The DMR reaction also produces syngas with high CO/H_2 molecular ratios. It actually appears that the ratio is less than one due to the following competing reaction: [11]

$$CO_2 + H_2 \leftrightarrows CO + H_2O \qquad \Delta H°_{298} = +41 \text{ kJ mol}^{-1} \qquad (1.6)$$

Although the reaction is desirable, a major problem exists with coke deposition, leading to the deactivation of the catalysts [11, 21]:

$$CH_4 \leftrightarrows C + 2H_2 \qquad \Delta H°_{298} = +75 \text{ kJ mol}^{-1} \qquad (1.7)$$

$$2CO \leftrightarrows CO_2 + C \qquad \Delta H°_{298} = -171 \text{ kJ mol}^{-1} \qquad (1.8)$$

The study of a number of different metals as catalysts has shown that noble metal catalysts demonstrate a high reactivity for this reaction as well as exhibiting low susceptibility to coking, but their high cost and low abundance means that they are of limited use in industrial processes [20, 22]. Nickel-based catalysts have shown positive results in this reaction. However, the catalysts greatly suffer from readily coking and hence the catalyst becomes further deactivated [20]. It is therefore highly desirable to seek a catalyst that has advantages in the three following areas: high catalytic activity, low cost, low susceptibility to coking.

1.3 Selection of metal catalysts

The literature abounds with research efforts in finding suitable metal catalysts for the aforementioned reactions, particularly DMR [11]. The main features that the catalyst should offer are as follows: the use of lower temperatures and pressures as well as the catalyst's resistance to side reactions such as sintering, coking and sulphur poisoning [11, 21]. The major problem is to minimising the Boudouard reaction and methane cracking, which lead to coke formation; both those reactions can be catalytically enhanced by certain metal catalysts [11, 21].

A significant amount of research efforts have targeted noble metal and transition metal catalysts. Promising results on the catalytic activities were achieved but their costs inhibit their use [16, 22, 23]. Nickel-containing catalysts can be easily sintered and have shown good reactivity for the DMR reaction however they suffer greatly from high coking [24, 25]. The addition of certain noble metals such as Au or Pd to produce metallic or bimetallic catalysts

have minimised these side reactions without affecting the DMR reaction, but the high cost of noble metals make them impractical for industrial processes.

Cobalt, molybdenum and tungsten-containing catalysts have shown promising results, both in the DMR reaction and resistance to coking [26]. These catalysts exhibit reactivity comparable to noble metals for both DMR and SR, whilst having a much greater coking resistance than nickel-based catalysts [23, 27].

It has been reported that some catalysts are prone to deactivation by oxidation processes to form higher oxides of the metal [24, 25] as shown below:

$$Mo_2C + 5H_2O \leftrightarrows 2MoO_2 + CO + 5H_2 \quad (1.9)$$

$$Mo_2C + 5CO_2 \leftrightarrows 2MoO_2 + 6CO \quad (1.10)$$

These reactions are particularly likely to occur for a particular 'type' of the carbide. Molybdenum carbides exist in a number of different polymorphs and it has been consistently reported that the above oxidation reactions are prevalent when particular types of molybdenum carbides are employed [27].

1.4 Catalyst supports

Studies have shown that not only can the active component of catalysts affect the catalytic activity but also the support materials may also have a marked effect on reactivity [22]. The most popular studied supports are TiO_2, Al_2O_3, MgO and SiO_2. It is reasonable to assume that the type of support / metal catalysts has a significant effect on catalytic activity and stability [28]. Molybdenum carbide catalysts show greater stability on Al_2O_3 support whereas Pd typically shows greater stability on TiO_2 support [28].

1.5 Bimetallic carbide catalysts

Research has shown that the addition of a second metal to metal carbides to form mixed metal carbides can significantly alter the structure and activity of catalysts [13]. Furthermore, the molecular ratio of the second metal added also has a marked effect on the catalyst performance [12]. It has been found that the molybdenum carbide catalysts to which cobalt

was added at the oxide formation stage, showed an increase in catalytic activity for different ratios of cobalt. Cobalt/molybdenum atomic ratio of 0.67 (i.e. $Co_{0.4}Mo_{0.6}C_x$) seems to give the optimum activity [12, 13]. It has been suggested that as the Co/Mo ratio increases the amount of $CoMoO_4$ formed at the oxide formation stage increases too and subsequently the formation of MoO_3 decreases. This increase in activity has mainly been attributed to the increase in surface area due to the smaller atomic radius of the incorporated cobalt atoms [12, 13].

The mixed metal carbide $Co_{0.4}Mo_{0.6}C_x$ has shown the greatest catalytic activity for the reactions mentioned above, as well as having greater stability to side reactions. It is inferred from this that the Co/Mo carbide phase is the most active component of the solid catalyst, due to the promoting effects of the cobalt. At molar ratios greater than 0.67, the separation of cobalt from the Co/Mo carbide phase is facilitated, giving a mixture of cobalt metal and molybdenum carbide, which leads to a marked decrease in activity [12, 13].

1.6 Supported metal carbides catalysts

Many researchers have studied the effects of supports for enhancing the catalytic activity of metal carbides [29]. Results show that not only has the support material affected the activity of the solid catalyst, but the identity of the metals is also important [29]. The main difference in the supported catalysts' activities seems to be linked to the structural effects of the supports such as surface areas, pores volume and size, which affect the chemisorption abilities of the catalyst [11]. It has also been suggested that the support materials can also affect the stability of the metal carbides [11].

Support materials have a profound effect on the catalytic activities of metal carbides. This has been attributed to the mechanism of reaction on the surface of the catalysts [11]. The various supports can be categorised into two main groups: acidic and alkaline supports. With acidic supports, the DMR reaction is thought to progress via a Langmuir-Hinshelwood mechanism; whereas the basic support activates the CO_2, which is subsequently reduced by dissociated CH_4 species [30]. The mechanism of reactions is outside the scope of this report, but further details can be obtained from Fan *et. al.* [11] and Gallego *et al.* [31].

A number of studies have been carried out on TiO_2 supports [29, 32, 33]. There are three common forms of TiO_2: the metastable anatase and brookite and the stable ore rutile. Results indicate that there is scope for a more detailed study of TiO_2 as a support material but the

stability of such support needs to be considered before this can be done. The use of Al_2O_3 has been found to be successful as the support of these catalysts, as well as giving the highest activity when compared to other supports, and its relatively low cost makes this a better option [26, 34].

1.7 Synthesis and characterisation of catalysts and their precursors

The synthesis of Co/Mo carbides is achieved by the reaction of Co/Mo oxides with hydrocarbons at high temperatures. The main hydrocarbons used for this reaction were methane and ethane. However, research shows that longer chain hydrocarbons may lead to the formation of carbide catalysts which are also effective. Furthermore, the reactions with longer hydrocarbons take place at lower temperatures and the surface morphology effects can lead to better a catalytic activity for certain reactions. The catalytic activity is affected both by elemental composition and surface morphology, which in turn seems to depend on the method of synthesis. According to the literature data, the most common procedures for preparing high surface area Mo_2C catalysts seem to be the following reactions: gas-phase reactions of volatile metal compounds [35, 36], reactions of gases with solid-state metal compounds [37, 38], pyrolysis of metal precursors [39] and solution reactions [39, 40]. Most researchers seem to prefer the gas phase carburisation of Mo oxides [40, 41]. Recent studies have also suggested that the source of carbon and conditions of the reactions play an important role in the activity of catalysts due to surface effects.

Beta-molybdenum carbide-based catalysts (such as β-Mo_2C) are well-known to demonstrate excellent catalytic activity in a wide variety of reactions, such as the hydrogenation of benzene, the hydrogenolysis of alkanes, and alkane isomerisation [42, 43]. The β-Mo_2C phase was reported to be an orthorhombic crystal structure with the experimental lattice dimensions of a = 5.195 Å, b=6.022 Å, c = 4.725 Å [44]. Other studies reported that bulk Mo_2C forms a disordered, hexagonal crystal lattice (see Figure 1 below) in which the molybdenum atoms form a hexagonal close-packed array and the carbon atoms occupy one half of the octahedral interstitial sites in a random manner [42].

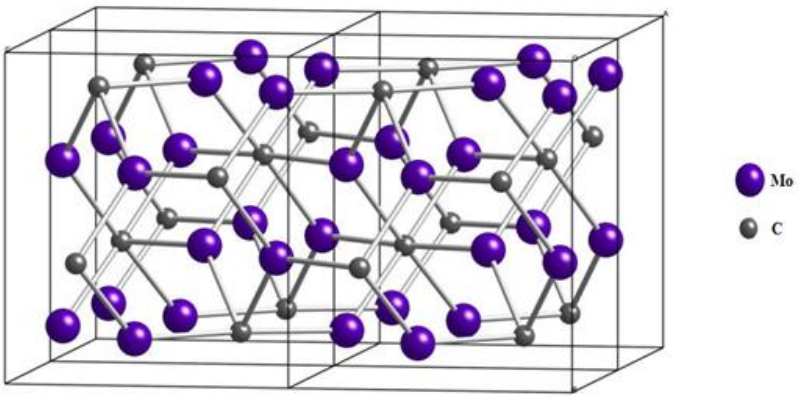


Figure 1: The crystal structure of Mo_2C [42, 43]

The starting material for catalyst synthesis, cobalt molybdate, $CoMoO_4$, (Figure 2), crystallises in the monoclinic structure [45, 46]. The unit cell has the following lattice parameters a = 9.67 Å, b = 8.85 Å, c = 7.76 Å, and β = 113^o 49` and contains a total of eight molecules. Oxygen atoms are six-fold coordinated around the cations in a close-packed arrangement of distorted octahedra based on the CoO type structure of the molybdates and cobaltates of small cations.

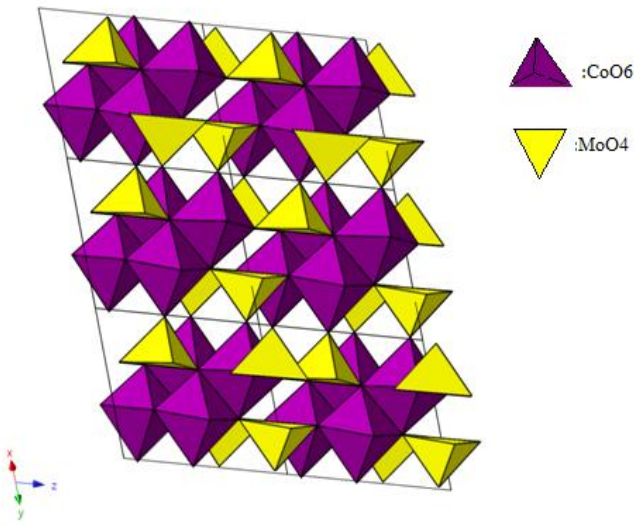


Figure 2: The crystal structure of $CoMoO_4$ [45, 46]

1.8 Catalytic activity

Mo_2C is known to catalyse some reactions such as steam reforming [47] and dry methane reforming [26]. Some studies have shown that these catalysts were stable at elevated temperatures and were also stable under normal conditions of temperature and pressure. In case of the supported carbide systems, it was found that γ-Al_2O_3 acted as the best support for stability and catalytic activity.

Bimetallic carbides of molybdenum and cobalt have been studied and have shown good stability and catalytic activity for the hydro-treatment process [48], mainly for the hydrodenitrogenation (HDN) reaction, but not for high-temperature reaction such as the dry reforming of methane. The present study extends this to the DMR reaction.

1.9 Aim of the project

The major objective of this project is to catalytically activate CO_2 and convert it into useful liquid fuels or chemicals by developing novel, non-precious metal-based multifunctional catalysts. We have specifically targeted molybdenum carbide and mixed Co/Mo carbides on a various support material. The effect of the preparation parameters' promoter and support material will be explored in an attempt to develop a catalyst with both high performance and high selectivity. Furthermore, the effect of reaction conditions will also be investigated, including experimental variables such as the molar ratio of the reactants, temperature, pressure and gas flow rates.

Chapter Two: Experimental Methods

All starting materials were used as bought from various suppliers without further purification.

The reaction scheme for catalyst synthesis is represented below:

$CoCO_3 + (NH_4)_6Mo_7O_{24}{\cdot}4H_2O$ [1]→ 'Salt' [2]→ Co/Mo Oxide [3]→ Co/Mo carbide

Where:

1 indicates the salt preparation for use as oxide forming precursor,

2 indicates the heat treatment to form the oxide, and

3 indicates the final carburisation process.

2.1 Chemicals

Co/Mo oxide and carbide samples have been synthesised using Co/Mo molar ratios of 0.67 [12, 48]. In the present study the starting materials used are: ammonium heptamolybdate $(NH_4)_6(Mo_7O_{24})\cdot(H_2O)_4$ (Sigma-Aldrich, 81.0-83.0% MoO_3 basis) and $CoCO_3$(Alfa-Aesar 99.5%), the support being γ-Al_2O_3(Alfa-Aesar). Samples of the oxides and carbides have been prepared as bulk solids as well as mixtures with the γ-Al_2O_3 support.

Additionally, for further clarity ammonium heptamolybdate $(NH_4)_6(Mo_7O_{24})$ $(H_2O)_4$ (Sigma-Aldrich, 81.0-83.0% MoO_3 basis) and $CoCO_3$(Alfa-Aesar, 99.5%) will be referred to as commercial chemicals. Finally, any oxide or carbide sample without any support (as shown in Sections 2.2.1 and 2.2.3 below) will be referred to as "bulk sample" in the remaining Sections of this thesis. Unless pointed out as commercially supplied, the samples in this these have been made by myself.

2.2 Preparation of Co/Mo catalyst

The catalysts in the present study have been prepared in a two-step process:

- Step 1 : The formation of the mixed Co/Mo oxide precursor, and
- Step 2 : The carburisation of the oxide under a controlled CH_4/H_2 atmosphere (achieved using carefully controlled flow rates, CH_4/H_2 ratio and reaction temperatures)

2.2.1 Preparation of $Co_{0.4}Mo_{0.6}O_x$

A series of supported bimetallic oxide samples ($Co_{0.4}Mo_{0.6}O_x$/ γ-Al_2O_3) have been prepared with the Co/Mo loading at 40 wt.% of Co/Mo oxide, whilst keeping the Co/Mo atomic ratio constant at 0.67 [12,13].

To a weighed sample of cobalt carbonate deionised water was added and the temperature was raised to 70°C. The mixture was stirred until all the salt had fully suspended in the water. To this suspension an excess of citric acid and dilute nitric acid was added and the mixture was stirred for five minutes to ensure a complete dissolution of the cobalt salt. To the resulting solution ammonium molybdate was added. The mixture was covered with cling film to minimise evaporation and left to stir overnight keeping the temperature at 100 °C. After this period, the temperature was increased to 105 °C and the cling film was removed; after that heating continued until all the water had evaporated, leaving a dark blue solid. This residue was placed in an oven at 600 °C to remove any water, ammonia, nitric acid and unreacted carbonate. After 10 hours under these conditions the product, a magenta coloured solid, was removed from the oven and allowed to cool down to room temperature.

The support material was prepared by annealing γ-aluminium oxide at 750°C for 180 minutes in air. The support material was then cooled down, added to the above solution and stirred for 120 minutes. The beaker was then transferred to an ultrasonic bath and left to run for a further 30 minutes. The resulting solution was then heated on a hot plate to remove the remaining water. After the removal of all water, the mixture was transferred to an alumina crucible and heated in a programmable tube furnace at a rate of 10°C/min to a maximum temperature of 600°C and kept at this temperature for 10 hours. The resulting solid was removed from the furnace, allowed to cool to room temperature and then finely ground with a

mortar and pestle. These samples were labelled "40% $Co_{0.4}Mo_{0.6}O_x/Al_2O_3$" which is covered in the discussion Section below.

2.2.2 Preparation of $CoMoPO_x$

The preparation details are as follows: $(NH_4)_6Mo_7O_{24}.4H_2O$ (Alfa Aesar, 99%) was dissolved in distilled water while adding H_3PO_4 drop wise and stirring until all the ammonium molybdate is fully dissolved. Citric acid was added to the solution while stirring to form a solution, then cobalt nitrate $Co(NO_3)_2.6H_2O$ was gradually added to the solution, stirred and heated to form a pink solution. The solution was statically placed in a sealed flask, and 2 days later, some white precipitation was seen and accumulated with time (the precipitation was believed to be a Co / Mo complex). The pink solution was filtered and the precipitate was dried to give the $CoMoPO_x$ sample, the Co to Mo ratio was controlled to 0.4 to 0.6 through the chemical added quantity.

2.2.3 Conversion from $Co_{0.4}Mo_{0.6}O_x$ to $Co_{0.4}Mo_{0.6}C_x$

The conversion of the above samples of Co/Mo oxides to the corresponding carbides was carried out in a quartz tube (internal diameter 9mm) with silicon wool support wads in a custom-designed furnace. The quartz tube containing the oxide samples was placed in the tube furnace which was located inside a fume cupboard. The quartz tube was connected to CH_4 and H_2 gas flow meters. The flow rates of CH_4 and H_2 were carefully adjusted so that a final volumetric ratio of CH_4/H_2 of 10% was achieved. The final total flow rate was 60 ml/min.

This setup (as shown in Figure 3 below) was heated from room temperature to 750°C at a heating rate of 3°C/min, then left at 750°C for three hours; and finally allowed to cool to room temperature under a continuous CH_4/H_2 flow.



Figure 3: The tube furnace used for conversion of Co/Mo oxides to the corresponding carbides, showing the quartz tube inside the furnace connected to supplies of CH_4 and H_2

2.3 X-ray powder diffraction (XRD) analysis

Powder XRD patterns were collected on a PW3040/60 X'pert PRO Console diffractometer using Cu-$K_{\alpha 1}$ incident radiation (1.5406 Å). The tube voltage was 45 kV and tube current was 40 mA. The scan diffraction angle was varied from 10º to 90º in 2θ and the samples were scanned at 0.008°/min in 2θ.



Figure 4: PW3040/60 X'pert PRO Console diffractometer.

2.4 Gas chromatography (GC) analysis

Gas chromatography (GC), as shown in Figure 5, is a widely-used analytic technique in many research and industrial laboratories for separating compounds based primarily on their volatilities. The sample is transported through the column by the continuous flow of an inert, gaseous mobile phase. The column itself contains a stationary phase, which is absorbed onto the surface of an inert solid. The main reason why different compounds can be separated by the GC technique is based on the interaction of a compound with the stationary phase. Put simply, the stronger the interaction, the longer the compound is attached to the stationary phase. Thus, the compound will take more time to transit through the column (i.e. the

compound has a greater retention time). The carrier gas must be chemically inert. Commonly-used gases include N_2, He, Ar, and CO_2.

- *Carrier gas*

The most critical characteristic of the carrier gas is for to be chemically inactive (i.e. inert). The type of the chosen carrier gas is usually dependent on the nature of the column and the type of detector used [49, 50].

- *Columns*

The most commonly-used columns are classified into two groups: packed columns and capillary columns. Packed columns are composed of a coil which is filled with the stationary phase. There are two general types of column, packed and capillary. Packed columns contain a finely divided, inert, solid support material coated with liquid stationary phase. Most packed columns are 1.5-10m in length and have an internal diameter of 2-4mm.

Capillary columns have an internal diameter of a few tenths of a millimetre. They can be one of two types; wall-coated open tubular (WCOT) or support-coated open tubular (SCOT). Wall-coated columns consist of a capillary tube whose walls are coated with liquid stationary phase. In support-coated columns, the inner wall of the capillary is lined with a thin layer of support material, onto which the stationary phase has been adsorbed. SCOT columns are generally less efficient than WCOT columns. However, both types of capillary column are more efficient than packed columns.

Phase polarity is the single most important characteristic in selecting a column because it dictates selectivity, or the ability of the column to separate sample components. Phase selection is based on the general chemical principle that "likes dissolves like." A non-polar column is best for the analyses of non-polar compounds. Polar columns most effectively separate polar compounds. Non-polar compounds are generally composed only of carbon and hydrogen atoms and contain carbon-carbon single bonds. Interaction between non-polar compounds and a non-polar phase are dispersive, meaning that they are governed by Van der Waals forces. Thus, larger compounds with higher boiling points have longer retention [49]. Elution order generally follows the boiling points of the compounds [50]. Polar compounds are composed primarily of carbon and hydrogen atoms, but also contain one or more hetero-atoms Intermediate polar or polar capillary columns separate polar compounds well.

In addition to dispersive interactions, interactions between polar compounds and the phase include dipole, pi-pi, and/or acid-base interactions. Separations are determined by differences in the overall effects of these interactions.

Polarisable compounds are compounds composed of carbon and hydrogen, but contain one or more double or triple carbon-carbon bonds. Highly polar capillary columns are generally used to separate these compounds.

- *Detectors*

Among different types of GC detectors, the flame ionisation detector (FID) and thermal conductivity detector (TCD) are the most commonly used detectors.

FID and TCD are characterised by high sensitivity to a wide range of components and both operate effectively over a wide range of concentrations. Their characteristics are summarised in the table below.

Detector	**Principle**	**Selectivity**	**Sensitivity (g/s)**
TCD	Measures the difference in thermal conductivity of gases	Universally responds to all compounds	10^{-10}
FID	Burns compounds in a H_2/O_2 flame at 2000˚C and measures the amount of ions created	Responds to all oxidable carbon compounds	10^{-12}

Table 1: Comparison of characteristics of GC detectors [49, 50]



Figure 5: Shimadzu GC-2014

2.5 Catalyst testing

Experiments were performed in a purpose-designed Micro-Reactor shown in Figure 6 (MicroReactor 10A, KLYT Catalysis Science & Technology Co., Ltd).

2.5.1 Variable temperature testing

For a kinetic and short-term stability test, samples have been tested in the micro-reactor under a temperature-programmed reaction. The catalyst bed was heated to 600°C under an inert N_2 atmosphere and atmospheric pressure with a temperature increase rate of 10°C /min, followed by a further increase up to 850°C at a rate of 5°C /min (see Figure 7). For a catalytic activity the reaction gases, for DMR studies, were passed through the reactor (35.6 % CH_4/ 35.6% CO_2/ 28.8% N_2) with a total flow rate of 40 ml/min. After 700°C the temperature was increased to 850 °C at a rate of 5°C /min and gas sampling injections were carried out every half an hour at 850 °C to test the activity, product selectivity and stability of the catalyst samples. The reaction was tested and calibrated with a mixed gas flow including a 1:1 ratio of CH_4/CO_2 and N_2, which is used as an internal standard. For each test the amount of catalyst used each time was 0.5000g ±0.0005g.

During the carburisation step the gas products were analysed using an on-line GC apparatus at every 50°C of increasing temperature.



Figure 6: The bench top MicroReactor 10A

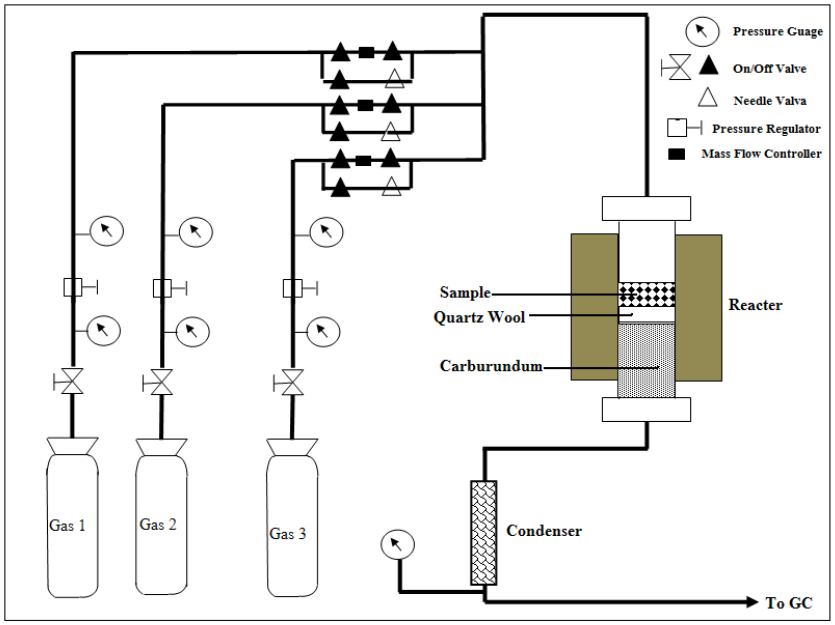


Figure 6.1: Schematic of the MicroReactor used in the catalyst evaluation in this work.

The conversion of CH_4 and CO_2 was calculated using an internal standard analysing method as shown by Liu *et al*. [51]. The total gas flow rate at the outlet of the reactor (F^{outlet}) can be calibrated using equation 2.1 as shown below:

$$F^{inlet} X^{inlet}_{Nitrogen} = F^{outlet} X^{outlet}_{Nitrogen} \quad \text{(For mass balance)} \quad (2.1)$$

Where F and X represent the total gas flow rate and mole fraction, respectively. The methane conversion (Conv.) can be determined using [51]:

$$Conv. = \frac{F^{inlet} X^{inlet}_{Methane} - F^{outlet} X^{outlet}_{Methane}}{F^{inlet} X^{inlet}_{Methane}} \quad (2.2)$$

$$= 1 - \frac{X^{outlet}_{Methane} X^{inlet}_{Nitrogen}}{X^{inlet}_{Methane} X^{outlet}_{Nitrogen}}$$

2.5.2 Catalyst stability studies

Stability tests were carried out in the apparatus described above and experimental procedures were in line with the methods described earlier. Typically, samples weighing 0.5g were used and the reactor tube loaded as described in the Sections above. Under a flow of inert N_2 (40 ml/min) and atmospheric pressure, the reactor was heated at a rate of 10 °C/min up to 850 °C (see Figure 8). When reaching this temperature the gas flow was switched to a mixture of 35.6% CH_4 / 35.6% CO_2 / 28.8% N_2 with a total flow rate of 40 ml/min. The reaction was allowed to continue for 300 minutes at this temperature, with samples being taken for analysis every 30 minutes. After 300 minutes of reaction time the reactor was allowed to cool to room temperature under a nitrogen gas flow rate of 40 ml/min. Once cooled down to room temperature, and passivated with static air for two days, the spent catalyst was collected.

With measured GC response for N_2, CH_4, H_2, CO and CO_2, the conversion of CH_4 and CO_2 was calculated and the selectivity was decided. The product ratio of H_2/CO was determined and the conversion-time profile plotted. The stability of the catalyst is easily determined from the graphs obtained [24, 34, 52].

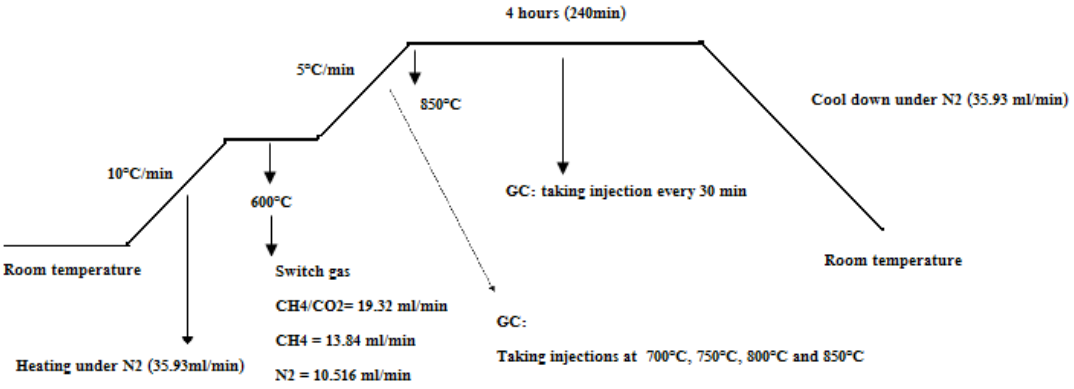


Figure 7: A typical variable temperature setting for the catalyst test.

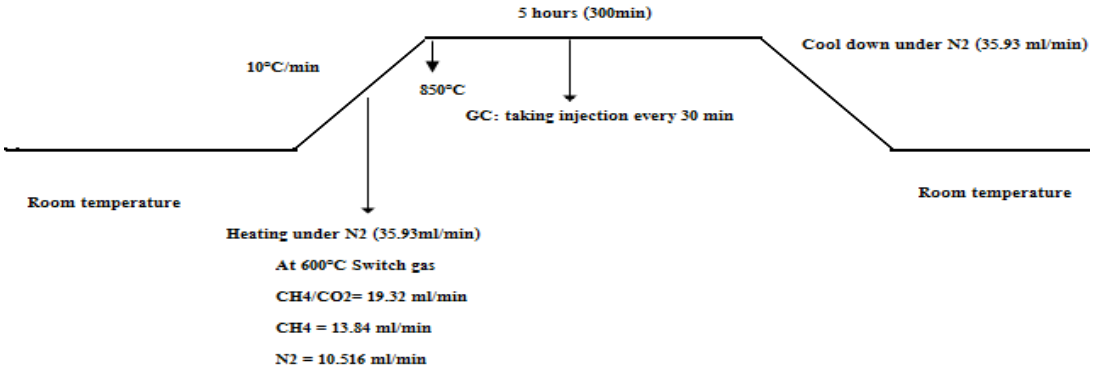


Figure 8: A typical catalyst stability test of the reactor condition setting.

Chapter Three: Results and discussion

3.1 Characterisation of materials

3.1.1 Oxides

XRD analysis is typically carried out to characterise any compositional change that occurs during the synthesis of catalysts and their catalytic testing. This analysis can be readily used to elucidate the existence of Co/Mo oxides and carbides, or more specifically the transformation of oxides to carbides.

Almegren *et al*. [48] has published data for X-ray diffraction analyses of bimetallic (Co/Mo) oxides, carbides, sulphides and nitrides. Xiao *et al*. [12] and Cheng *et al*. [53] both have presented data for mono-metallic Mo, Co/Mo oxides and carbides. Similarly, Wang *et al* [54] have presented data for XRD analysis of bi- and mono-metallic compounds for bulk unsupported Mo and Mo compounds with γ-Al_2O_3 support. In those papers, Cheng *et al*. [53], and Wang *et al*. [54] both have described how MoO_3 was prepared from $(NH_4)_6(Mo_7O_{24}).(H_2O)_4$.

The XRD powder pattern in Figure 9 shows the results obtained in the present work using variable temperature XRD analysis of $(NH_4)_6(Mo_7O_{24}).(H_2O)_4$ samples. It is believed that changes in the structure of the starting material occurred as indicated by the appearance and the loss of several peaks. A multi-step chemical transformation, the first step of which consists of the loss of four water molecules can be evidenced from the appearance of four new peaks between the temperatures of 197.8˚C and 247˚C (at 2 theta angles of 17˚, 19˚, 30˚ and 35˚). The second step of this reaction is the loss of NH_3 and finally the last step is the conversion to molybdenum trioxide at a temperature of 297°C.

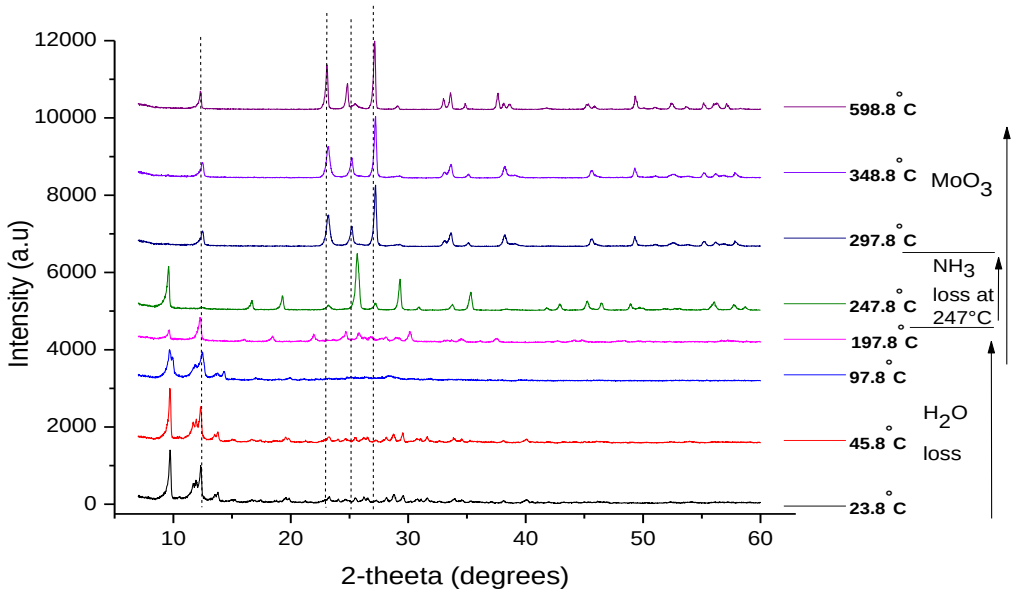


Figure 9: Variable temperature X-ray powder diffraction patterns of $(NH_4)_6Mo_7O_{24}{\cdot}4H_2O$.

Figures 10 and 11 below show the results for the XRD analysis of bulk MoO_3 samples, both from experiments and literature data. After comparing both patterns, it is clear that MoO_3 has been successfully synthesised.

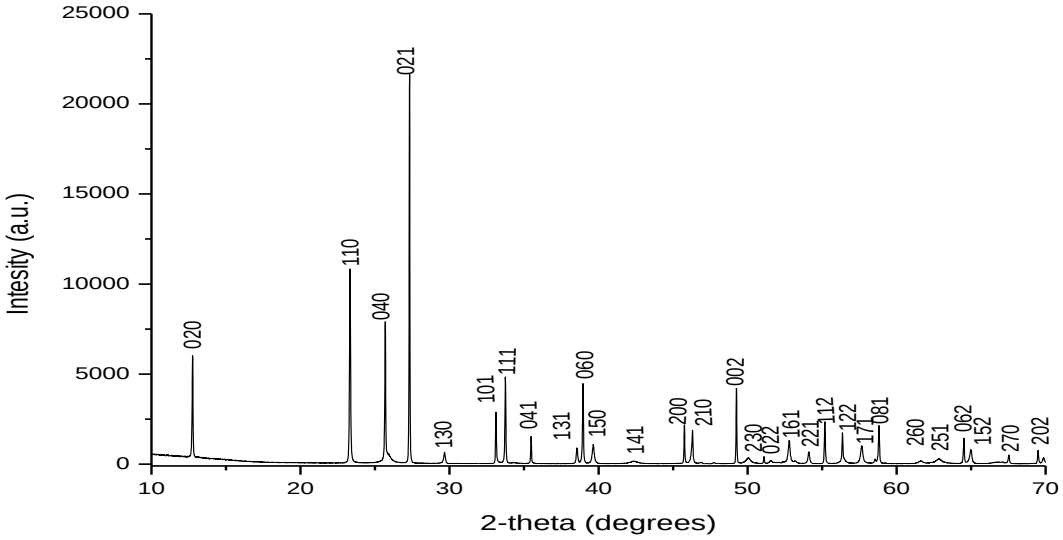


Figure 10: X-ray powder diffraction pattern of MoO_3 bulk material synthesised by heating ammonium heptamolybdate at 600°C.

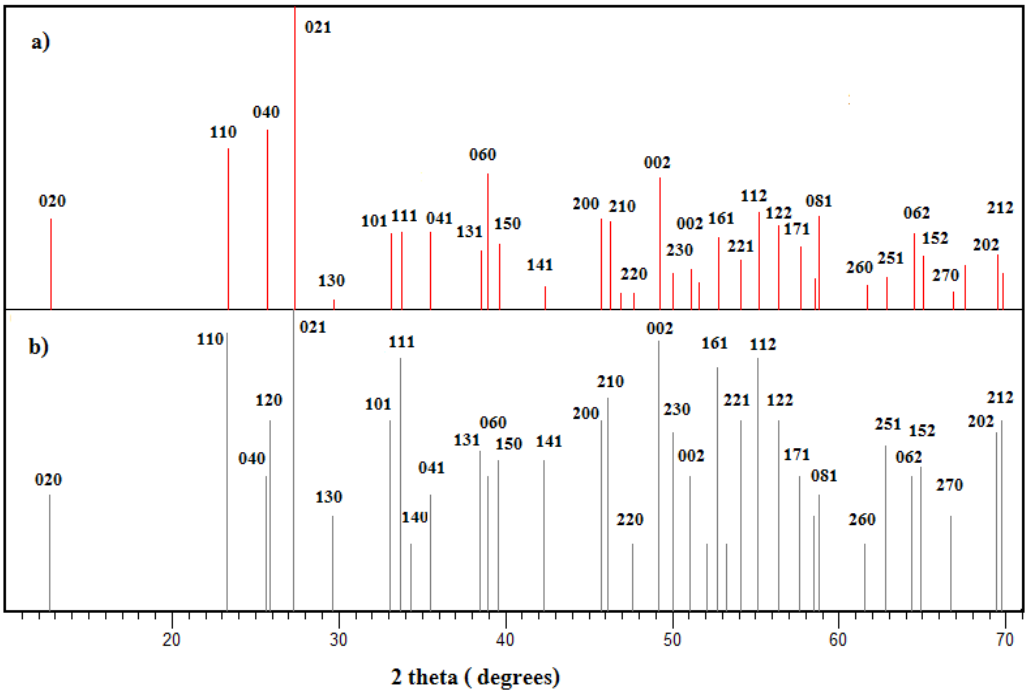


Figure 11: X-ray analysis of (a) MoO_3 bulk [present study] and (b) from Leisegang *et.al*. [55].

Figures 12 and 13 below show the XRD patterns for a Co_3O_4 bulk sample synthesised from the decomposition of $CoCO_3$ The results indicate that after annealing of $CoCO_3$ at 600°C for 10 hours the corresponding oxide Co_3O_4 has been formed. This can be evidenced from the coincidence of the peaks in the spectra, which strongly suggests that Co_3O_4 has been successfully formed. A further comparison with published works [56, 57] indicates that the transformation to Co_3O_4 has been successfully carried out.

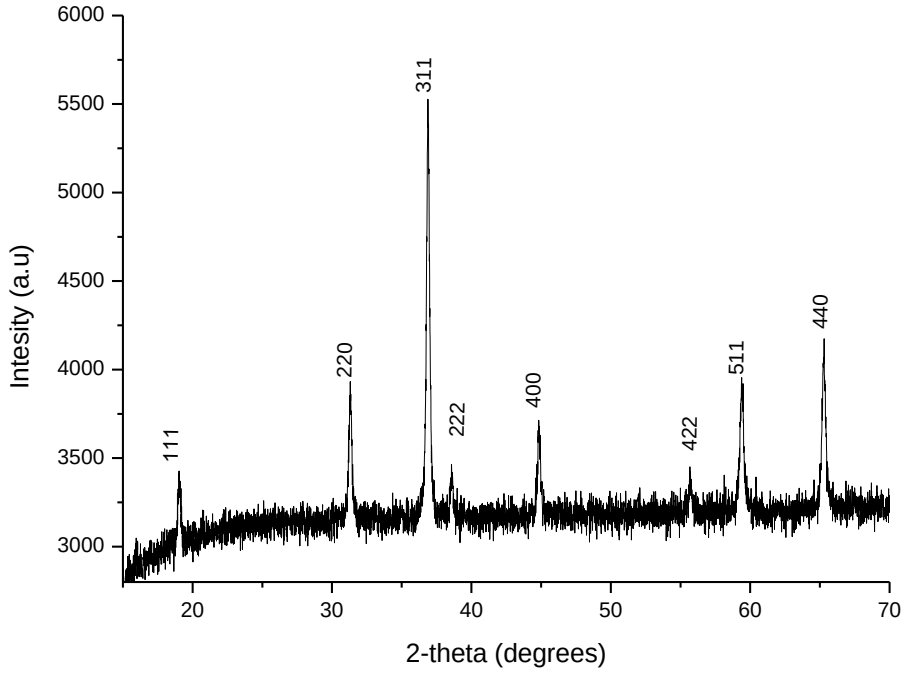


Figure 12: X-ray powder diffraction pattern of Co_3O_4 bulk sample after calcination of $CoCO_3$, at 600°C for 10 hours.

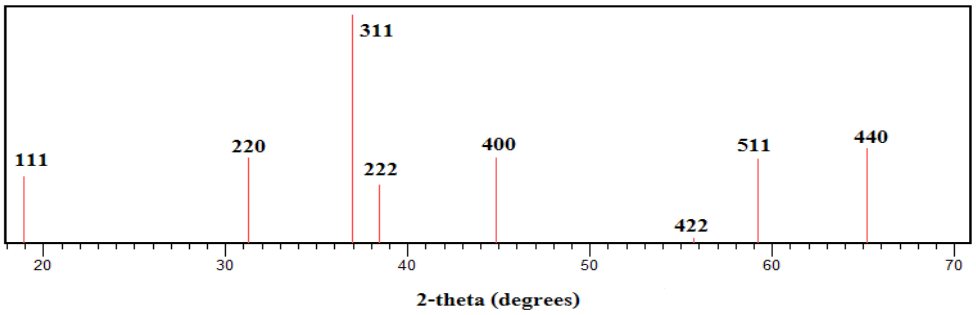


Figure 13: X-ray pattern for the Co_3O_4 bulk from Will *et. al*. [58].

Figure 14 (below) shows the results obtained from the XRD analysis of the $Co_{0.4}Mo_{0.6}O_x$ sample supported by γ-Al_2O_3 and prepared in the present study. Additionally, Figure 15 shows the XRD spectrum of γ-Al_2O_3 (supplied by Alfa-Aesar) and supported Co/Mo oxides. The broad peaks at circa 46° and 67° can be assigned to γ-Al_2O_3, whereas the strong peaks between 23° and 33° are attributed to the Co/Mo oxide. We consider that the other peaks come from the overlap of peaks from both solids. Those results are in good correlation with several published articles, as evidenced by the works of Wang *et al* [54] and Korlann *et al*.

[59]. Some peaks with Miller indexes [112], [131], [204] and [441] (Fig. 14) have not been identified and are believed to be artefacts.

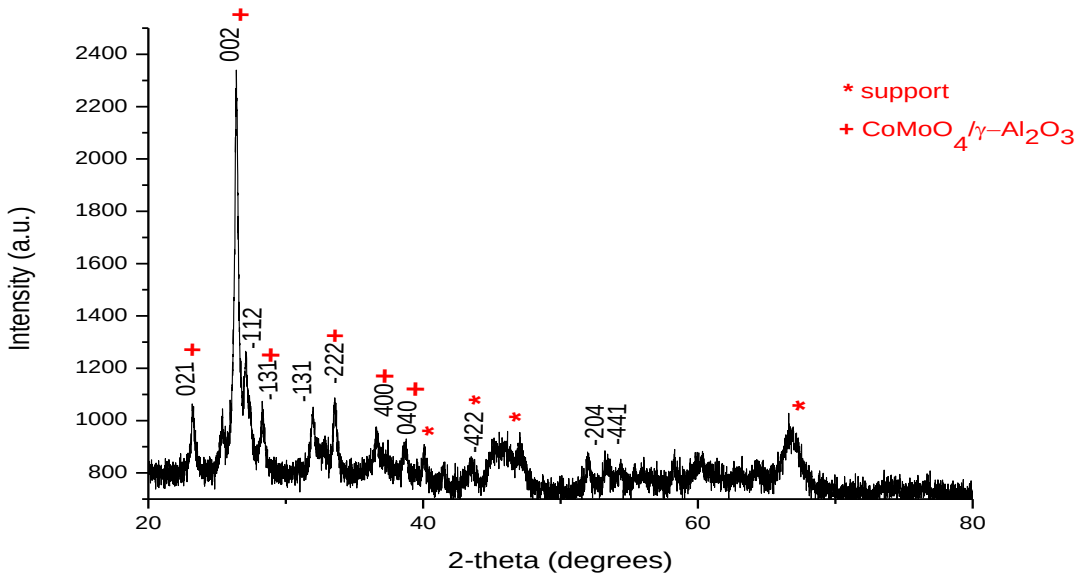


Figure 14: X-ray powder diffraction pattern of $Co_{0.4}Mo_{0.6}O_x/\gamma\text{-}Al_2O_3$ after mixing $CoCO_3$, $(NH_4)_6Mo_7O_{24}.(H_2O)_4$ with $\gamma\text{-}Al_2O_3$ and followed by calcination at 600°C for 10 hours. $\gamma\text{-}Al_2O_3$ support peaks are represented as asterisks.

The XRD patterns displayed in Figure 15 are both for $\gamma\text{-}Al_2O_3$ supplied by Alfa-Aesar and $(Al_2O_3)_{0.9}(Mo_{1-x}Co_xO_z)_{0.1}$ bimetallic supported oxides (where x = 0.2, 0.4, 0.6 and 0.8). The patterns clearly show the broad peaks for the alumina at around angles of 38°, 46° and 67° and a broad peak between angles of 20° and 30°, which appears in the $(Al_2O_3)_{0.9}(Mo_{1-x}Co_xO_z)_{0.1}$ samples only. This broad peak at 20° - 30° can be attributed to the finely dispersed Co/Mo oxide phase as indicated in Figure 15 below.

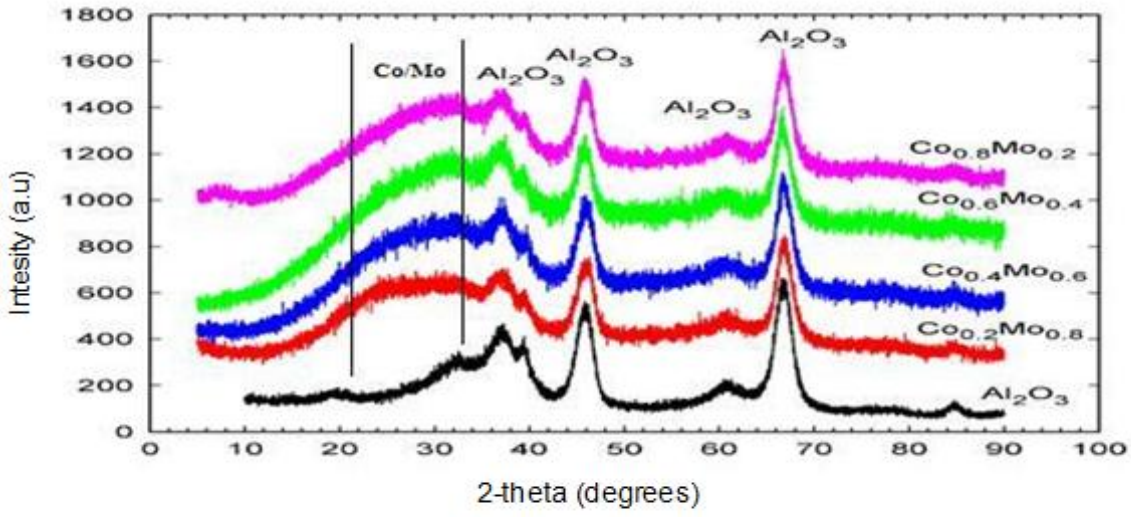


Figure 15: X-ray powder diffraction spectra of γ-Al_2O_3 and $(Al_2O_3)_{0.9}(Mo_{1-x}Co_xO_z)_{0.1}$ bimetallic supported oxides with x = 0.2, 0.4, 0.6 and 0.8. The broad peak between 20° and 30° arises from the Co/Mo oxide phase.

3.1.2 Carbide

Both the XRD patterns of molybdenum carbide prepared in this study and molybdenum carbide prepared and characterised in the literature are presented in the Figure 16 and Figure 17 below. The comparison of these patterns with that of the transformed molybdenum carbide prepared in the laboratory (Figure 17a), indicates that the carbide has been successfully synthesised after carburisation of MoO_3 in a CH_4 /H_2 mixture. Those results are believed to be in good agreement with data published by Cheng et al. [53] and Wang et al. [54].

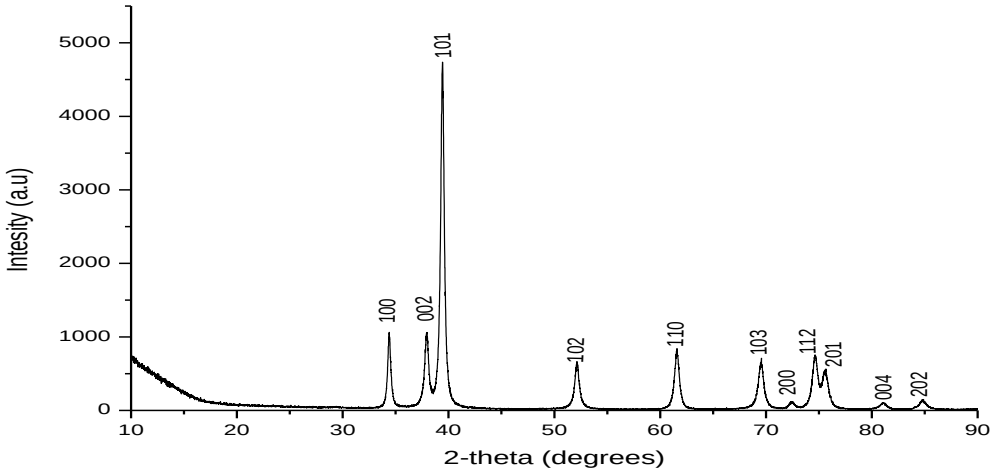


Figure 16: X-ray powder diffraction patterns of Mo_2C bulk sample after conversion from MoO_3.

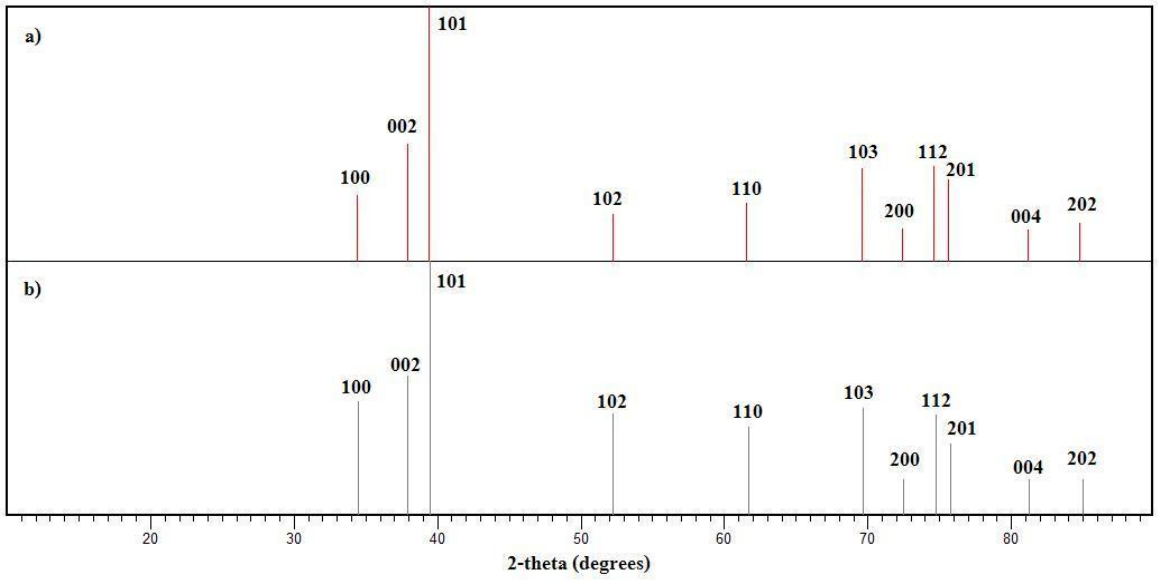


Figure 17: The X-ray analysis pattern a) of Mo_2C bulk [present study] and b) from Page *et al*. [43].

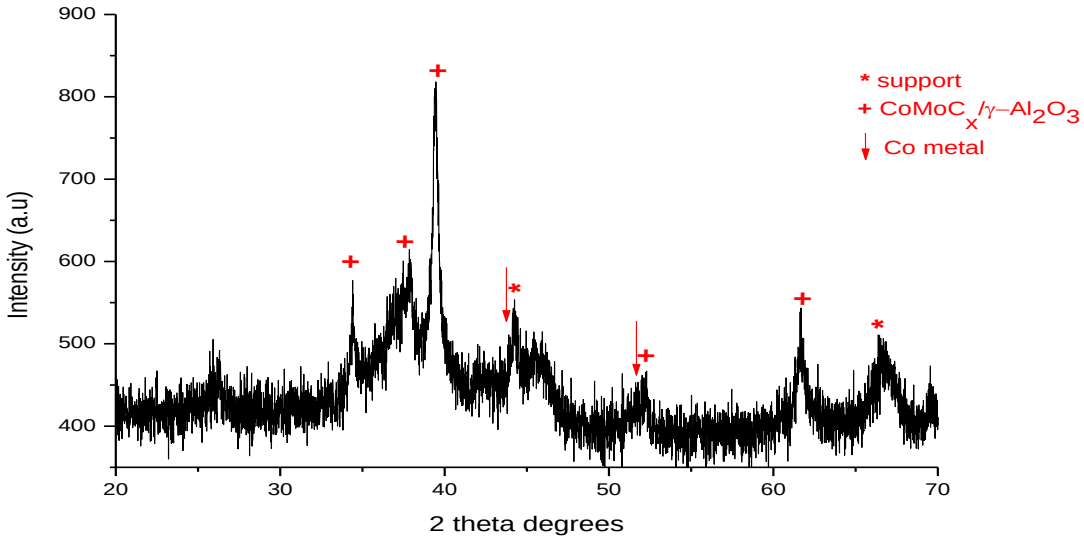


Figure 18 X-ray powder diffraction pattern of $Co_{0.4}Mo_{0.6}C_x/\gamma\text{-}Al_2O_3$.

Figure 18 above shows the results obtained from the XRD analysis of the supported $Co_{0.4}Mo_{0.6}C_x/\gamma\text{-}Al_2O_3$ sample prepared in the present study. The broad peaks between 34° and 45° can be attributed to the Co/Mo carbide. Other peaks can be attributed to the overlap of peaks from both solids. However, no peaks which can be attributed to the Co metal have been detected. The results are in good agreement with the data published in the literature as mentioned in the papers of Xiao *et al*. [12] and Almegren *et al*. [13, 48].

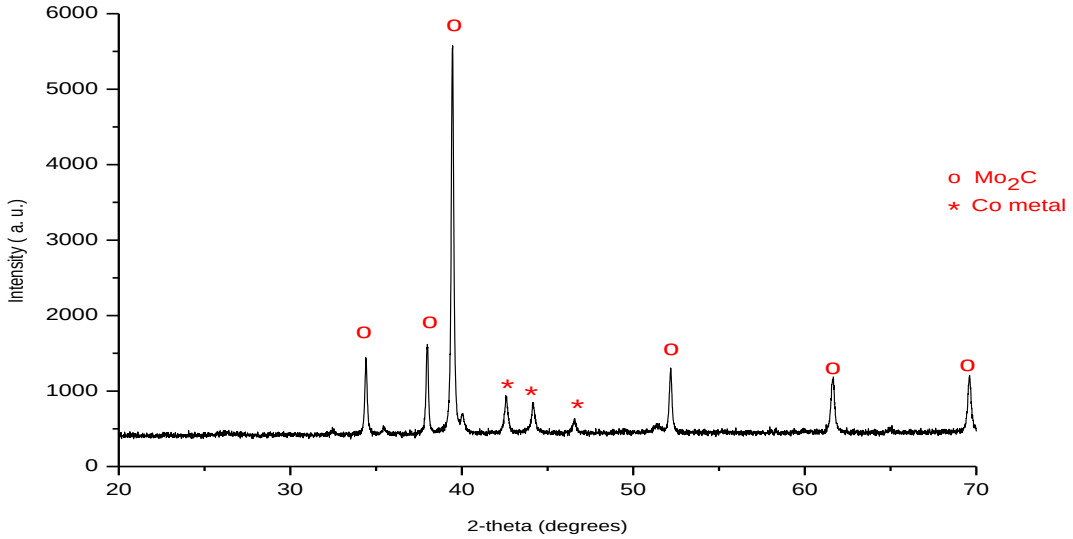


Figure 19 X-ray powder diffraction pattern of $CoMoPC_x$.

In figure 19 above shows the results obtained from the XRD analysis of the $CoMoPC_x$ sample prepared in the present study. The patterns clearly show the peaks for the Mo_2C at around angles of 34°, 38°, 39° , 52° , 61° and 69° at a 2θ [43]. However, metallic cobalt particles have been detected, as marked with the *.

3.2 Catalytic tests

The main aim was to obtain novel bimetallic catalysts that could be used for transforming the two greenhouse gases CO_2 and CH_4 to compounds that would be useful for liquid fuel and at the same time reducing their concentration in the atmosphere (for a certain period). The series of experiments carried out in this research project have principally tested the stability of the catalysts towards temperature and their effectiveness in the DMR reaction (equation 1.5).

Since the DMR reaction has a high positive enthalpy of reaction, it is favoured by high temperatures; and we would expect the conversion to increase as the temperature increases. Another important reaction that may occur during these tests is the RWGS reaction

(Equation 1.5).A further reaction that may take place during the catalytic tests is shown in equation 1.7.

The results will be discussed in the Sections below and the relative importance of these reactions further compared.

3.3 Stability of catalysts with temperature

3.3.1 Stability of bulk catalysts

A number of the produced catalysts have been tested under the experimental conditions previously described in Section 2.5.1 above. The materials chosen for testing are the bulk carbides and 40% mixed Co/Mo carbides.

As previously described in Chapter 2, the CH_4 and CO_2 conversions have been calculated using an internal standard method. The results for the methane-derived carbides are given in Figure 20 to Figure 22 below.

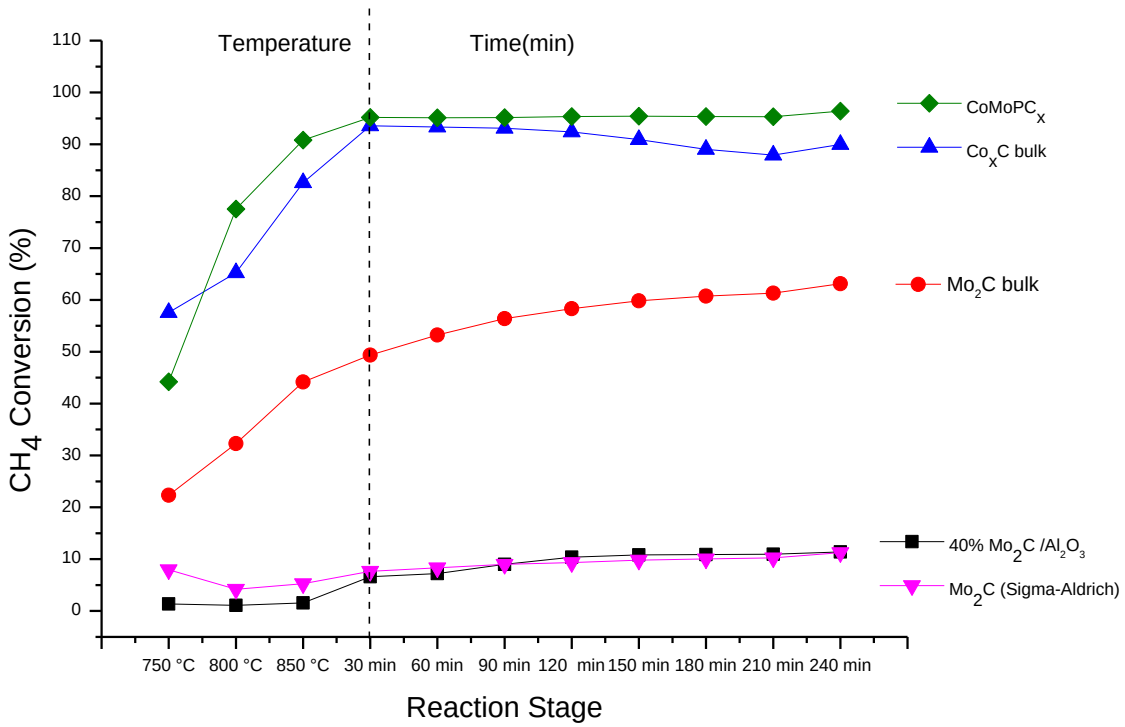


Figure 20: CH_4 conversion during the variable temperature studies of bulk mono and bimetallic carbides and one supported catalyst.

Figure 20 presents the CH_4 conversion for bulk carbides samples under the variable temperature studies. The data for $CoMoPC_x$ show that the percentage of CH_4 conversion sharply increases from 40% to about 90% when temperature rises from 750°C to 850°C. As

the temperature is kept constant at 850°C, the activity remains high at about 95% indicating that the sample is stable at this temperature for the whole duration of the test (i.e. 240 minutes).

The graph for the Co_xC bulk sample shows an increase in activity with temperature (from about 60 % conversion of CH_4 to about 85%). As the temperature is kept constant at 850°C the activity remains high at circa 95% and relatively stable.

The activity of the Mo_2C bulk sample is also shown in Figure 20 above and it can be seen that the catalytic activity at 750 °C starts at about 22% and increases to about 45% at a temperature of 850 °C. The temperature was then maintained at 850 °C over the whole period of the test and the activity demonstrates a steady and constant rise with time, to finish at about 60% CH_4 conversion after the duration of the experiment. The lower conversion at the temperature below 850 ^oC is due to the oxidation of the carbide by CO_2, which is the active site for CH_4 decomposition. When the temperature rises to 850 ^oC, the oxidized catalyst surface may be re-carburised, thus leading to higher activity.

The results also indicate that for Mo_2C supplied by Sigma-Aldrich and 40% Mo_2C/Al_2O_3 the activity is significantly lower than for the other samples. The methane conversion rate at a temperature of 750 °C started at around 10% and rose slowly with time. It is interesting to note that both those samples show no increase and at times, even decrease in activity when temperature increases.

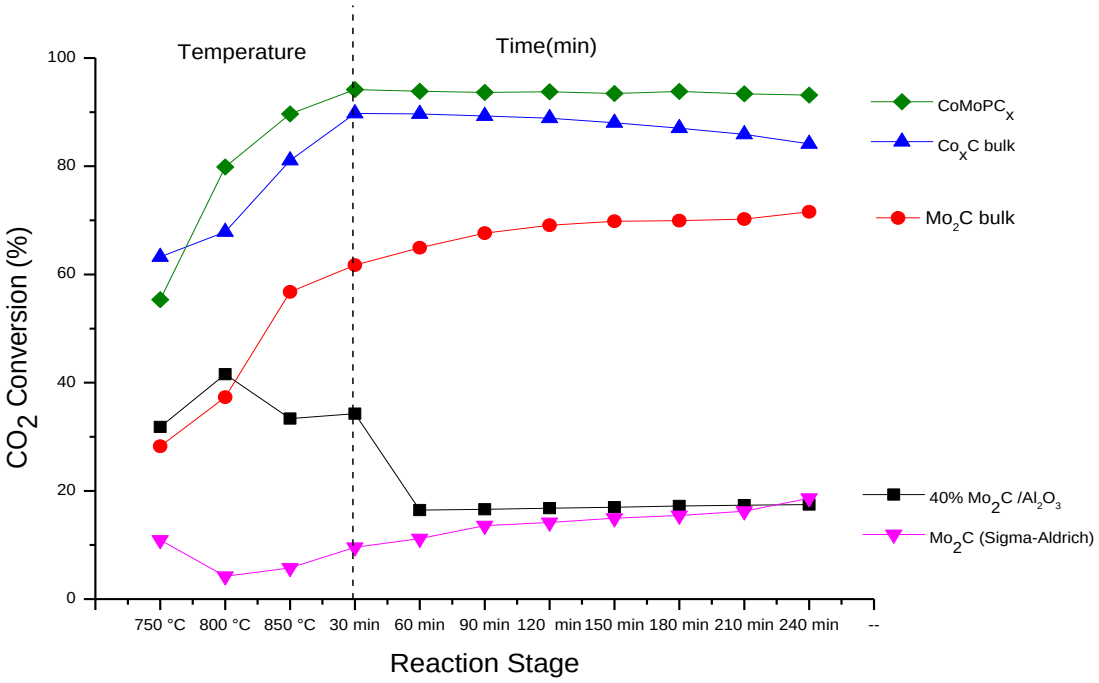


Figure 21: CO_2 conversion during the variable temperature studies of bulk carbides and one supported catalyst.

Studies of the CO_2 conversion show that both $CoMoPC_x$ and Co_xC (bulk) follow a similar pattern in their activities. Both samples display high initial CO_2 conversion rates at around 60% for temperatures of 750°C and reach over 90% conversion when the temperature is increased to 850°C. The conversion activity is maintained for the whole duration of the test as shown in Figure 21 above. This strongly indicates that the samples are stable at a temperature 850°C for the test period of 240 minutes.

Conversion results for the Mo_2C (bulk) show that the activity is raising from about 25% to nearly 60% as the temperature increases from 750°C to 850°C. This conversion activity is then steadily maintained for the whole duration of the test, meaning that no further change in CO_2 conversion occurs with time.

The 40% Mo_2C/Al_2O_3 has an initial increase in activity from 30% to over 40% conversion rate when the temperature is increased from 750°C to 800°C. This is followed by a gradual loss in activity to around 30% at a temperature of 850°C. After a reaction time of 60 minutes at 850°C, the conversion activity sharply decreases to about 15% and then remains constant for the whole duration of the test.

The activity of the Mo_2C supplied by Sigma-Aldrich starts at a low level (about 10%) and slightly decreases in activity to about 5% when the temperature reaches 800°C. The CO_2 conversion rate is returned to its initial levels after 60 minutes at a temperature of 850°C and slowly increases for the whole duration of the test. At the end of the test - at 240 minutes - a sudden rise occurs, which might suggest that the conversion has not reached its peak and might carry on for longer than the test duration. Further investigation is then needed to confirm the above.

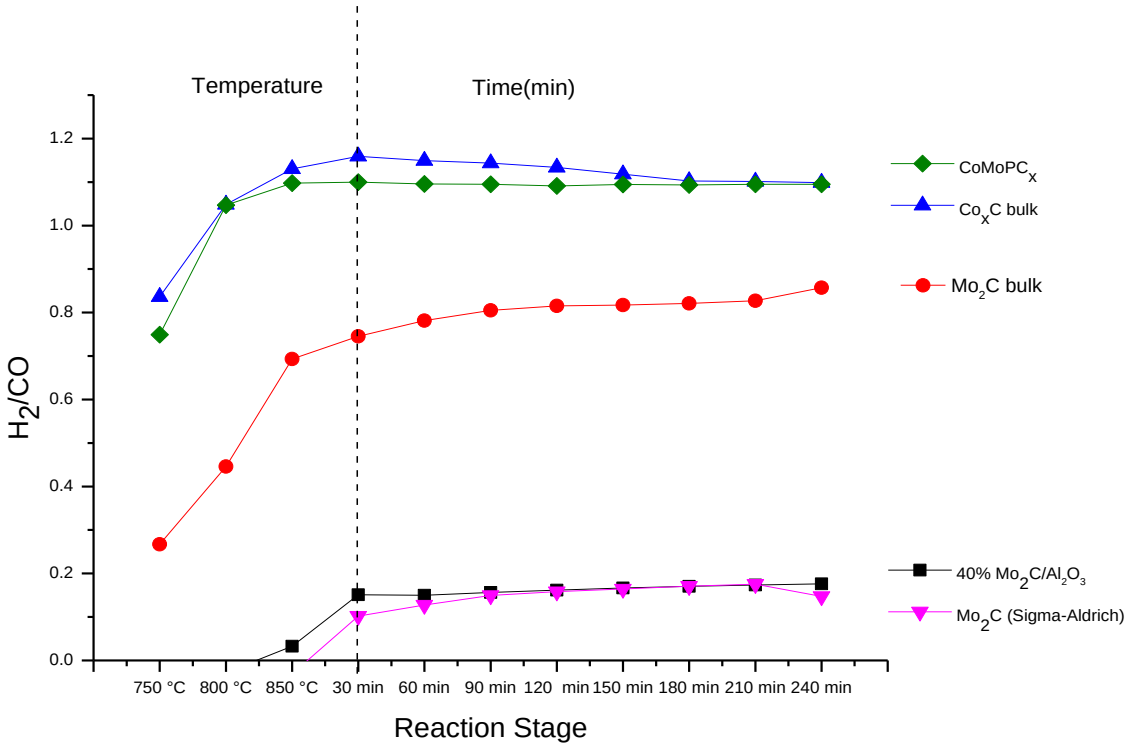


Figure 22: Dependence of the reaction product ratio (H_2/CO) over reactions time for bulk carbides and one supported catalysts.

The results presented in Figure 22 above show that the molar ratio of H_2/CO for $CoMoPC_x$ and Co_xC (bulk) is about 1:1. We consider that this is indicative of a good conversion rate (as shown in Equation 2.3, Section 2.5) for the DMR reaction. The H_2/CO molar ratio for Mo_2C bulk catalyst is circa 0.6, which strongly suggests that the RWGS reaction is becoming more prominent. We also note that very low molar ratios of H_2/CO conversions have been achieved for both Mo_2C and the bimetallic carbide.

The results shown in Figure 20, 21 and 22 above indicate that for unsupported catalysts $CoMoPC_x$ and Co_xC show significant activity. This activity is typically maintained at a temperature of 850°C for the whole duration of the test. It is noted that both conversion rates of CH_4 and CO_2 can be considered high.

Mo_2C (bulk) shows some activity, however it is not as significant as the other catalysts studied in our experiments. From our experimental results, we can possibly suggest that at both high and lower temperatures, Mo_2C bulk is only about half as active as both CoC_x and $CoMoPC_x$ as evidenced in Figures 20, 21 and 22. Similarly, Mo_2C (bulk) shows higher activity at elevated temperatures indicating that it is less effective at temperatures lower than 850°C. The greater activity at higher temperature could be related to the fact that the reaction

under study is endothermic and thus, would be thermodynamically favoured at higher temperatures.

At the beginning of the experimentation at temperatures of 750°C, both Mo_2C supplied by Sigma-Aldrich and the 40% Mo_2C/Al_2O_3 show little to no activity in the region of about 3%. This result shows that the conversion reaction is not simply depending on higher temperatures of 850°C i.e. significant amounts of catalysts are needed before the conversion reaction is initiated.

The DRM reaction produces both H_2 and CO in the molar ratio of 1:1. It is expected that our experimental results should similarly achieve a molar ratio of 1:1 for the H_2/CO conversions. Any deviations from this theoretical result might indicate that other reactions are also taking place concomitantly. It has been evidenced that the RWGS reaction may occur during the DMR reaction if the favourable conditions of temperature and concentration are met. This would result in the production of additional CO and simultaneously, the levels of H_2 would start to decrease leading to an overall molar ratio of less than 1:1.

If the carburisation reaction in which the methane is broken down to C and H_2 takes place, we would expect the molar ratio of H_2/CO to increase above 1. Furthermore, the deposition of C on the catalysts would lead to a significant loss of catalytic activity.

It is noted that the molar ratio of H_2/CO for $CoMoPC_x$ and Co_xC is close to 1:1, which strongly indicates that the DMR reaction is the main reaction taking place. The molar ratio is then further maintained from the duration of the whole test, which then demonstrates the chemical stability of the catalysts under high temperatures.

3.3.2 Stability of supported catalysts

A number of the produced supported catalysts were tested under the conditions previously described in Section 2.5.1 above. The materials chosen to undergo the testing were the supported bimetallic Co/Mo carbides and Co_xC/γ-Al_2O_3.

The CH_4 and CO_2 conversions for both the supported bimetallic Co/Mo carbide and Co_xC are given below in Figure 23 and Figure 25 respectively.

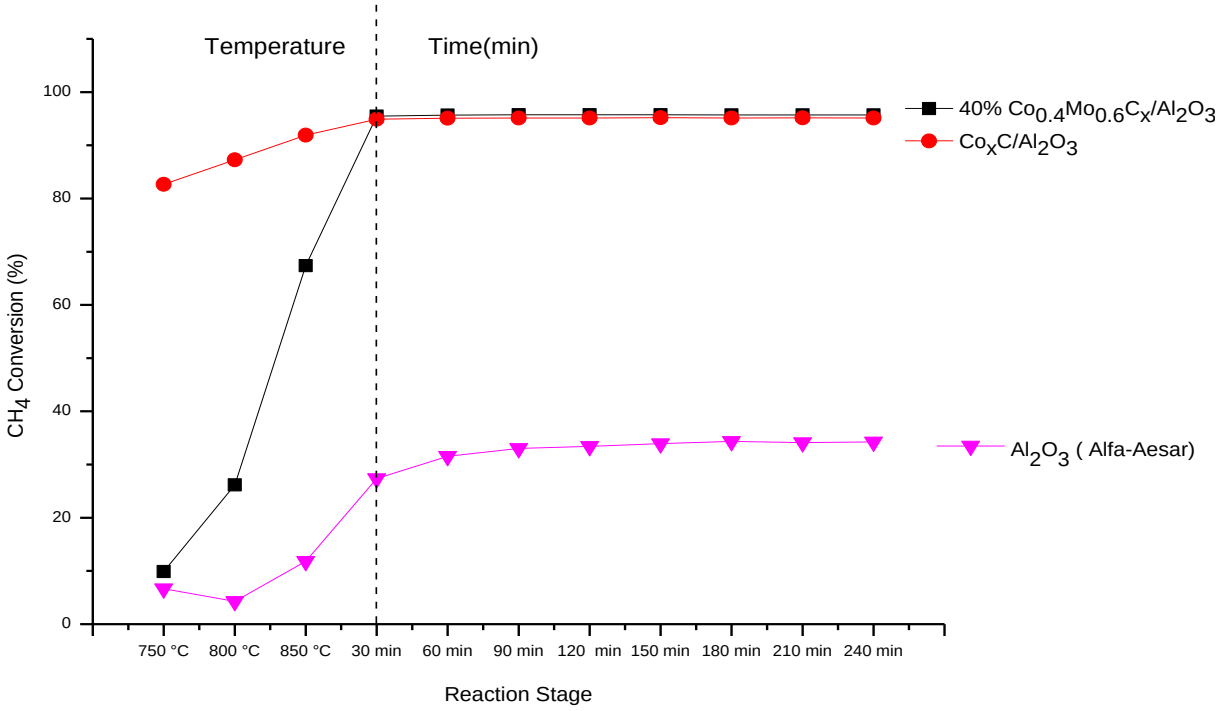


Figure 23: CH_4 conversion during the variable temperature studies of γ-Al_2O_3 (Alfa-Aesar) and γ-Al_2O_3-supported carbides.

In Figure 23 the Co/Mo carbide on support (γ- Al_2O_3) shows a sharp increase in activity (from 10% to 95%) when temperature increases from 750°C to 850°C. Furthermore, this high activity is maintained for the duration of the test (i.e. 240 minutes).

For the 40% Co_xC/γ-Al_2O_3, the activity at a temperature of 750°C is about 80% and the CH_4 conversion increases to about 95% at a temperature of 850°C. The activity is then maintained at this level for the whole duration of the test.

Tests related to the activity of the support (γ-Al_2O_3) supplied by Alfa-Aesar show that there is small variation between temperatures of 750°C and 850°C after 30 minutes. Similarly, little or no increase has been noted with time with the final CH_4 conversion activity levelling at about 30% as demonstrated in Figure 23 above.

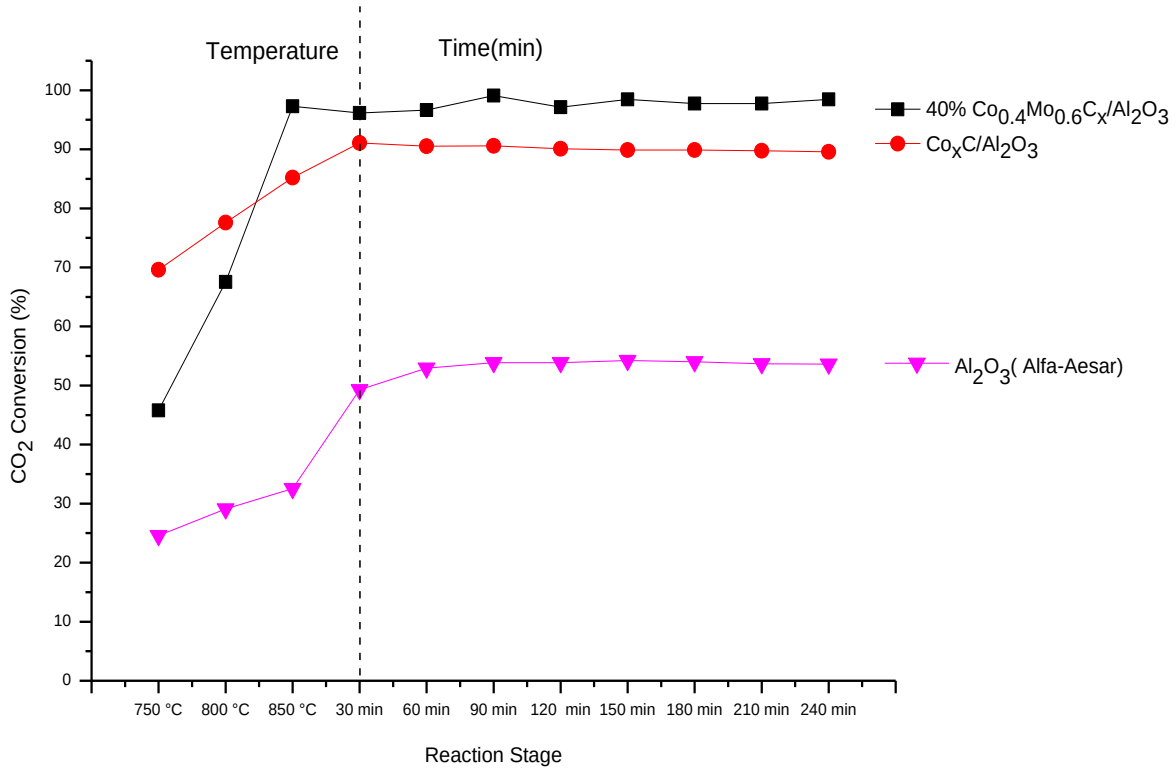


Figure 24: CO_2 conversion during the variable temperature studies of γ-Al_2O_3 (Alfa-Aesar) and γ-Al_2O_3-supported carbides.

In Figure 24 the conversion of CO_2 for the bimetallic carbide on support shows a significant increase in activity, from 45% to 95% when temperature increases from 750°C to 850°C. This activity is then maintained for the duration of the test. Cobalt carbide on support shows a small increase in activity from 70% to about 90% when the temperature is increased from 750°C to 850°C. The activity is then maintained for the duration of the experiment. Additionally, the support itself shows some reduced activity from around 20% to 50%, however it is not as significant as with the carbides. After an initial increase, the activity is maintained slightly below 50% for the rest of the experiment.

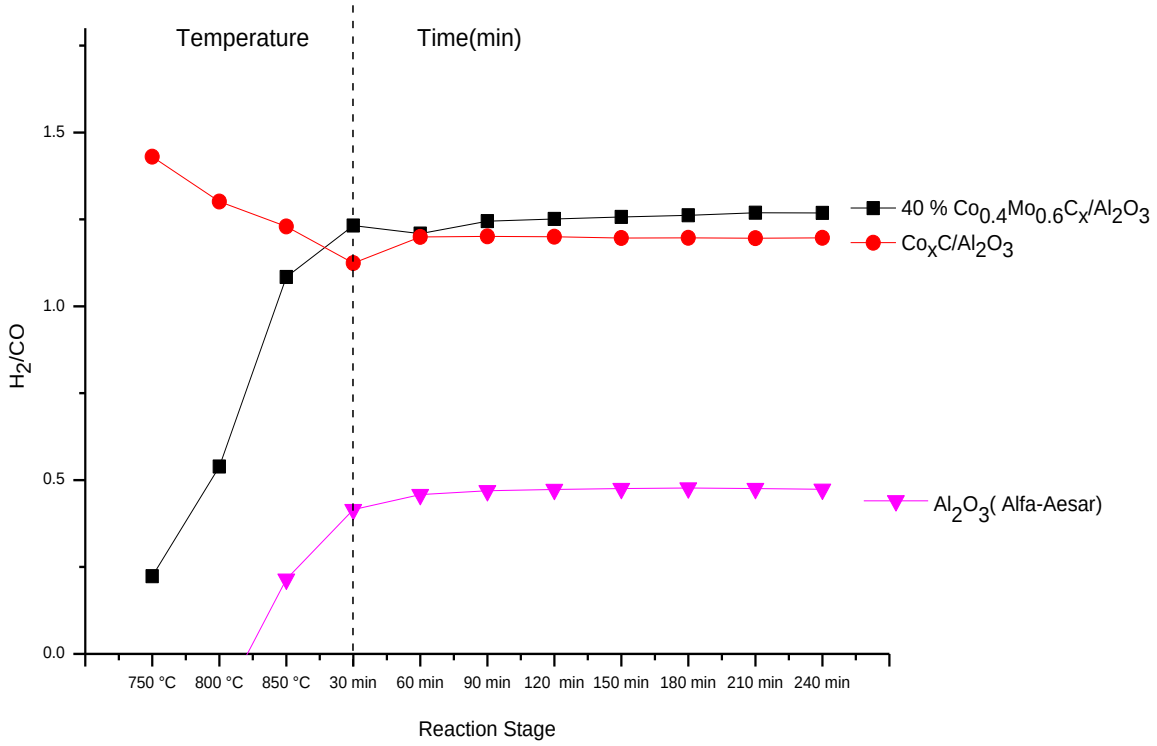


Figure 25: Dependence of the reaction product ratio (H_2/CO) on reactions time for supported carbides.

The data shown in Figure 25 indicate that the ratio of H_2/CO conversion for the bimetallic carbide is 0.25 at 750°C and reaches a level of about 1.1 at a temperature of 850°C. This strongly indicates that a good conversion for the DMR reaction can be obtained under those conditions. It is worth mentioning that the high H_2/CO ratio of 1.5 observed at 750°C for Co_xC on support falls to about 1.1 at a temperature of 850°C. The support γ-Al_2O_3 shows a low ratio of H_2/CO conversion of about 0.4, however.

The ratio of CH_4 conversions to CO_2 conversions and the product ratio of H_2/CO on different catalysts are shown in Figure 25 above. On each material chosen in this figure, the conversion ratio of CH_4/CO_2 is always higher than the product ratio, which means that a side reaction, the Reverse Water Gas Shift (RWGS), is probably occurring during the DRM process. Compared with the results of supported carbides, the differences between the conversion ratio of CH_4/CO_2 and the product ratio on bulk carbides and carburised support are significantly higher. This might suggest that a high level of the RWGS reaction is probably occurring with these two materials. Hence, according to the all results above, the support effect cannot only make an apparent higher conversion of both CH_4 and CO_2 but can also decrease the extent of the RWGS side-reaction which occurs on the catalysts.

The results presented in the Figures 23, 24 and 25 indicate that for both supported bimetallic Co/Mo carbides and Co_xC, a higher catalytic activity has been be achieved. This activity is then maintained for the whole duration of the experiment showing that the catalysts are stable at temperatures up to 850°C. Figure 25 shows that for Co_xC the H_2/CO ratio is significantly higher than (1.25) for temperatures lower than 850°C, which tends to suggest that the RWGS reaction may also be occurring under these conditions. However, it appears that this reaction becomes less significant with time as the conversion rate stabilises at 1.25 for the duration of the experiment.

γ-Al_2O_3 is the most widely used support for catalytic carburisation due to its outstanding textural and mechanical properties and its relatively low cost [60]. However γ-Al_2O_3 can also become fairly unstable at high temperatures. Several studies have shown that it is possible to synthesise highly stable Al_2O_3 that offers high surface area [61]. If surface area does not vary drastically after high-temperature treatments, a phosphorous-containing catalyst (such as $CoMoPC_x$) with a more convenient texture can be obtained. For instance, Montesinos-Castellanos [62] have shown that a high surface stable alumina support is able to support Mo particles with different volume / surface ratios.

3.3.3 Catalysis stability tests

3.3.3.1 Stability of catalysts with time

A number of the produced catalysts were tested under the conditions previously described in Section 2.5.2 above. The materials chosen for the testing were the bulk carbides and bulk 40% Co/Mo carbides.

The CH_4 and CO_2 conversions for both bulk carbide samples are given in Figure 26 and Figure 27 respectively. Due to the time taken for the gas mixture to stabilise, we have decided to discard any of the results collected before the experiment time reached 30 minutes.

From the results exposed in Figure 26 below, it seems rather clear that both $CoMoPC_x$ and Co_xC (bulk) show good stability for the whole duration of the test (i.e. 300 minutes). After 5 hours at 850°C both materials show an almost identical and almost constant activity of near 100% for CH_4 conversion.

However, the Mo_2C sample shows a constant fall in activity, and hence stability, decreasing from an initial activity of 95% to around 40% after 5 hours. We consider that the test needs to be extended to see whether the decreasing trend continues with time.

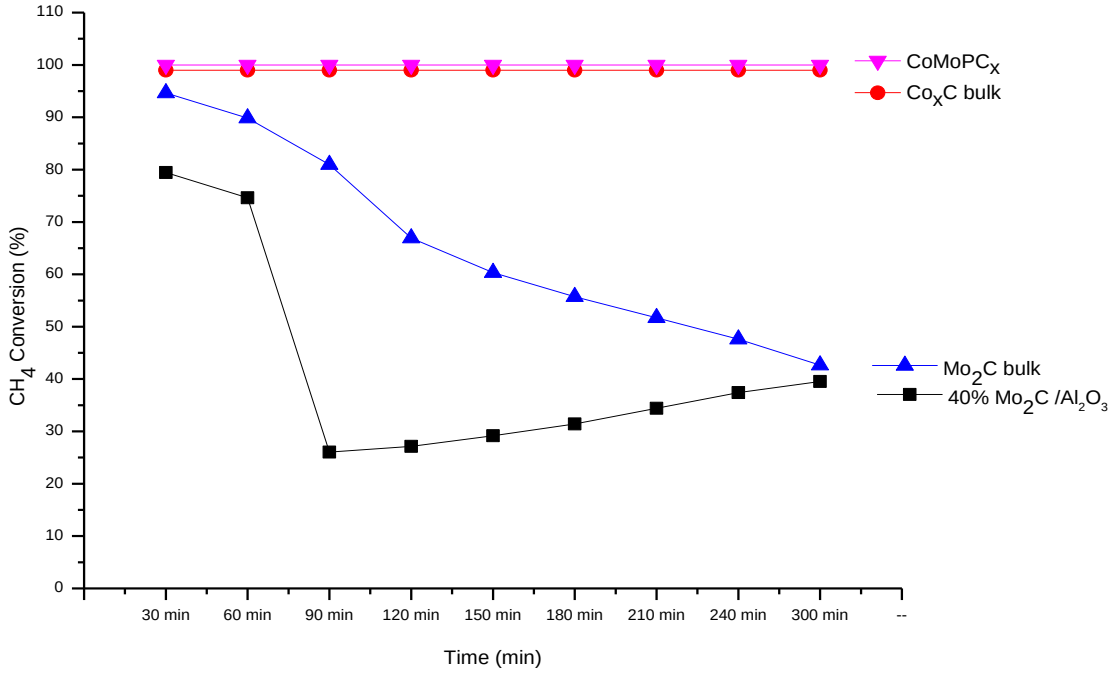


Figure 26: CH_4 conversion during the stability studies of bulk carbides and one supported catalysts at 850°C.

Finally, the results indicate that for the Al_2O_3 supported Mo_2C catalysts, there is a sharp initial drop in activity from 80% to 25% and then from around 90 minutes, the activity steadily increases to reach a final activity level of 40% after reaction time of 300 minutes. It is believed that further investigation is also needed to conclude on the CH_4 conversion activity levels of the Co/Mo carbide.

In Figure 27 below displays the CO_2 conversion results. Our data show that both $CoMoPC_x$ and Co_xC (bulk) have a high activity of around 90% throughout the test duration; whereas the Mo_2C bulk and supported sample shows increasingly poor stability results since the CO_2 conversion activity steadily drops from high initial levels of over 90% to significantly lower levels of 45%.

Similarly, the bimetallic carbide activity shows a sharp decrease, from 90% to 40% after about 90 minutes. This is then followed by a constant and steady increase to reach an activity level of 55% after 300 minutes of reaction test.

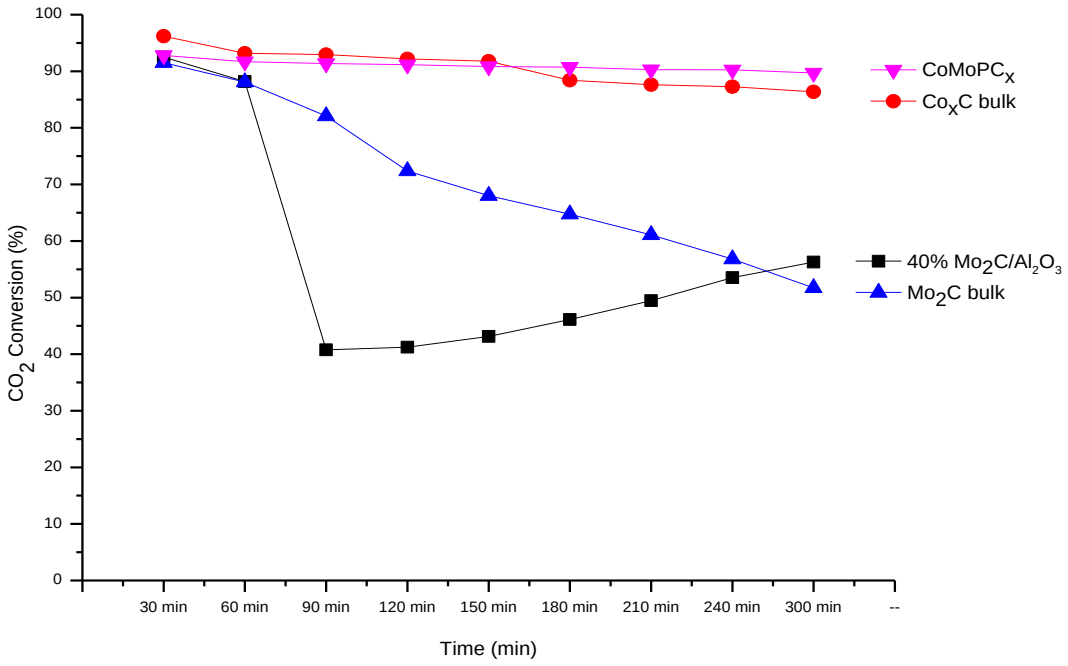


Figure 27: CO_2 conversion during the stability studies of bulk carbides and one supported catalysts at 850°C.

$CoMoPC_x$ was used as a comparative catalyst. In Figure 28 below, $CoMoPC_x$ shows the highest molar ratio of H_2/CO at a value of 1.2, indicating good experimental conditions for the DMR reaction and less preferable conditions for the RWGS reaction. As such, we can deduce that $CoMoPC_x$ is the best catalyst for the DMR reaction compared to Co_xC bulk, Mo_2C bulk and 40% Mo_2C/Al_2O_3

The activity of bimetallic carbide follows the similar trend as exposed in Figures 28, starting with a sharp decrease from 0.85 to around 0.45 after 90 minutes followed by a steady and constant rise to around 0.55 after 300 minutes of reaction.

Additionally, the Co_xC sample shows a constant increase in H_2/CO molar ratio from 1.0 to about 1.1, indicating that the RWGS reaction is occurring to a lesser extent after a reaction time of 150 minutes, and some excessive methane decomposition may occur. Finally, the H_2/CO molar ratio when testing the Mo_2C bulk and the supported Mo_2C constantly decreases throughout the experiment showing a loss in activity with time.

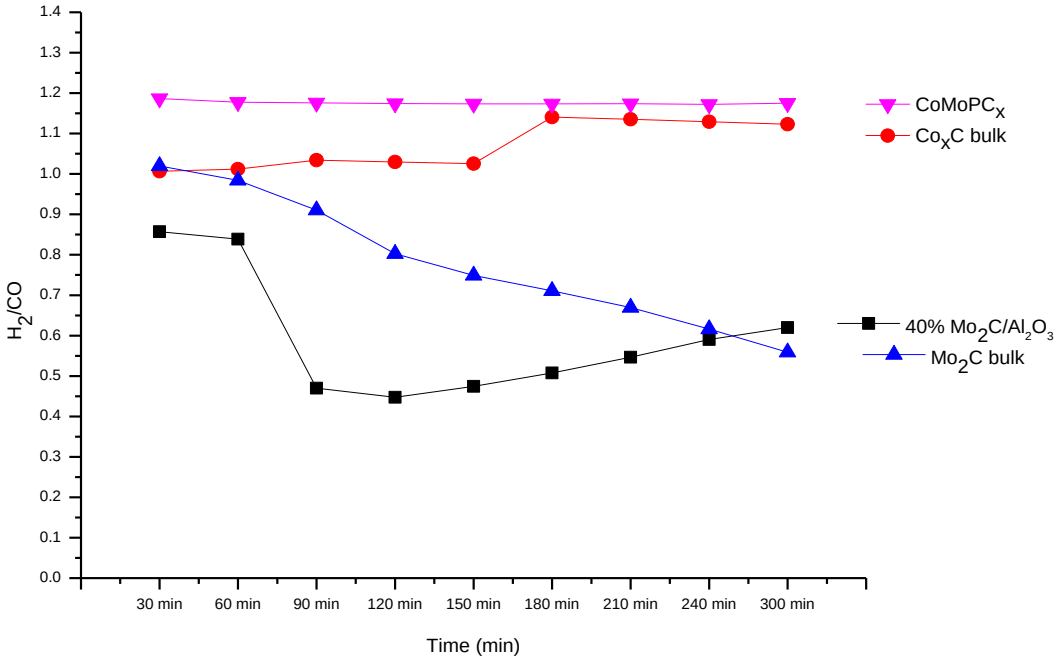


Figure 28: Dependence of the reaction product ratio (H_2/CO) on reactions time for bulk carbides and one supported catalysts at 850°C.

3.3.3.2 Stability tests of the supported catalysts

A number of the produced catalysts were tested under the conditions described in Section 2.5.2 above. The materials chosen for the testing were the supported bimetallic Co/Mo carbide, $Co_xC/\gamma Al_2O_3$ and 60wt% of Mo_2C/γ-Al_2O_3.

The CH_4 and CO_2 conversions for both supported bimetallic Co/Mo carbide, Co_xC and Mo_2C are given in Figures 29 and 30 respectively.

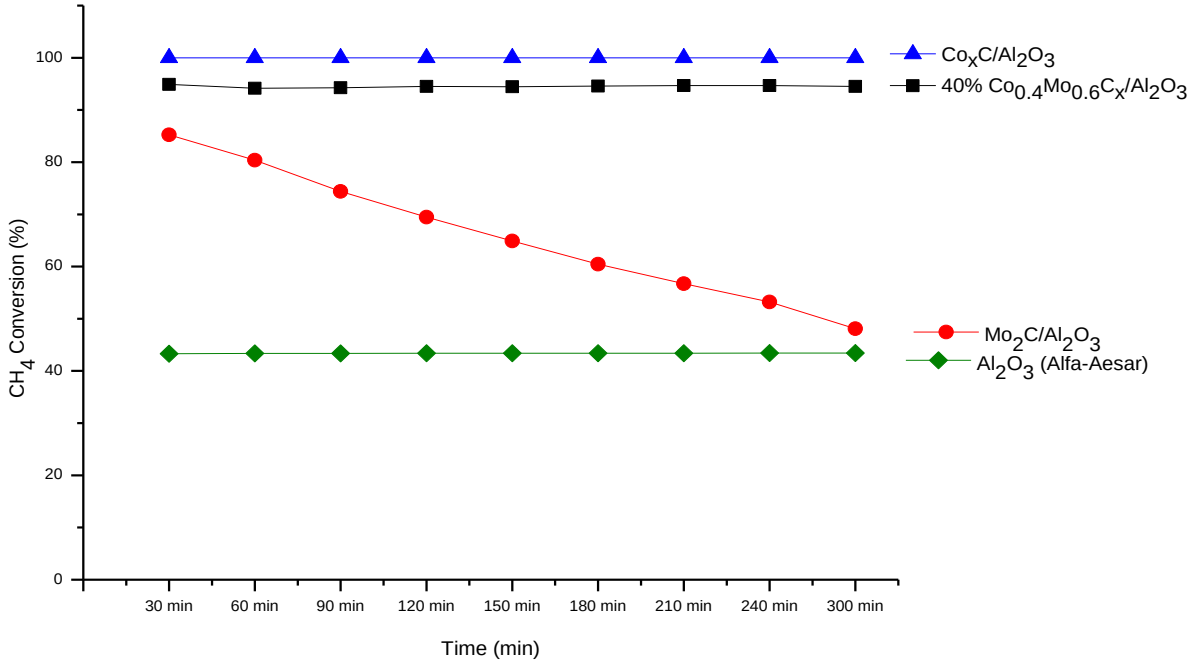


Figure 29: CH_4 conversion during the stability studies of γ-Al_2O_3-supported carbides at 850°C.

Figure 29 above shows that there is significant reactivity difference for the various samples under study, in terms of the methane conversion. For example, we note that the catalytic activity of the Al_2O_3-supported Mo_2C falls rapidly with time; whereas for the other three samples there is almost no change in the conversion of methane for the duration of the experiment. This may be due to the way how Mo_2C behaves at high temperatures, whereas the change for the other catalysts is not as pronounced at similar temperatures. Our experiment also demonstrated that despite the quite high catalytic activity of bimetallic carbide, it can be considered slightly less active than the supported Mo_2C or the Co_xC samples. This may be due to the surface effects, which occur at the surface of the support during the formation of the bimetallic carbides.

These results show that the bimetallic carbides and Mo_2C samples are very stable at these temperatures with respect to their catalytic activity. It is evident that the molybdenum carbide sample does suffer from loss in catalytic activity. However, the other two samples show maintained high catalytic activity at high temperature for about 300 minutes.

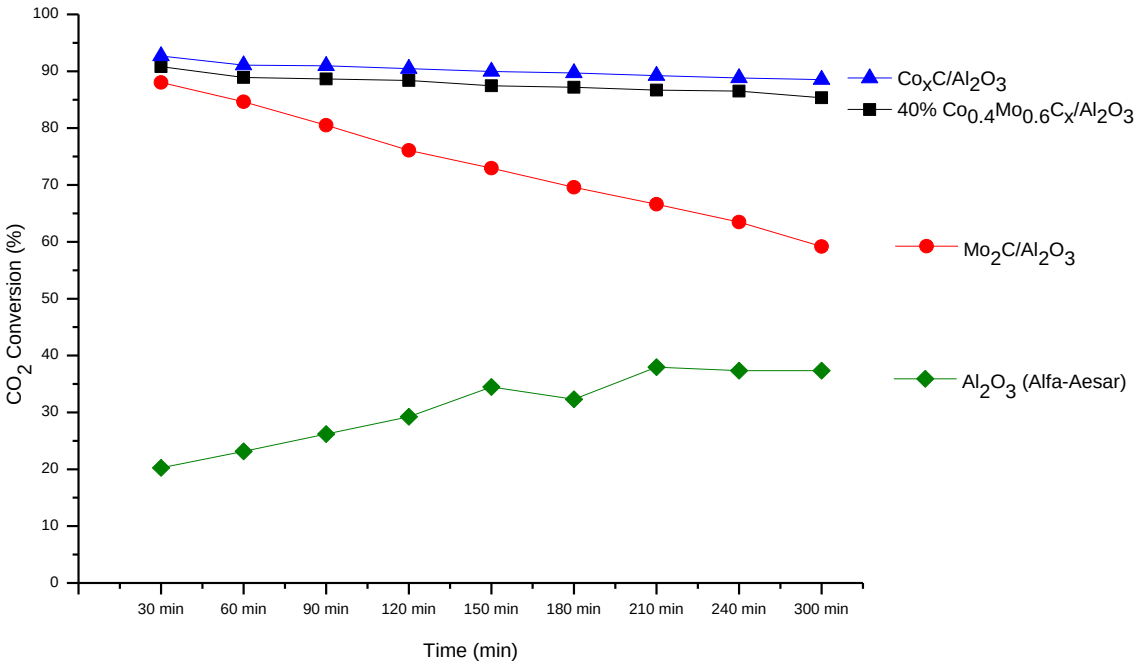


Figure 30: CO_2 conversion during the stability studies of γ-Al_2O_3 (Alfa-Aesar) and γ-Al_2O_3-supported carbides at 850°C.

Figure 30 above shows the results for the CO_2 conversion of bimetallic carbide, Mo_2C, Co_xC and Al_2O_3. We note that the stabilities of both Al_2O_3-supported Co/Mo and Co_xC catalysts are steadily kept at around 90% for 300 minutes of experiment. However, for Mo_2C/Al_2O_3 the CO_2 conversion drops from an initial figure of 90% down to 60% activity after 300 minutes of testing. The results show that there are clear differences in the conversion of CO_2 between the three catalysts and these differences become more pronounced with time. Both the bimetallic carbide and the Co_xC samples show a high level of activity, which is maintained with time. The Mo_2C catalyst shows an initial high activity which drops sharply with time, indicating a lack of stability under high temperature. Oppositely, the support Al_2O_3 shows a slight and constant increase in CO_2 conversion with time, indicating that at high temperatures the support may also lead to CO_2 breakdown due to the changes that may occur at the surface of the catalyst.

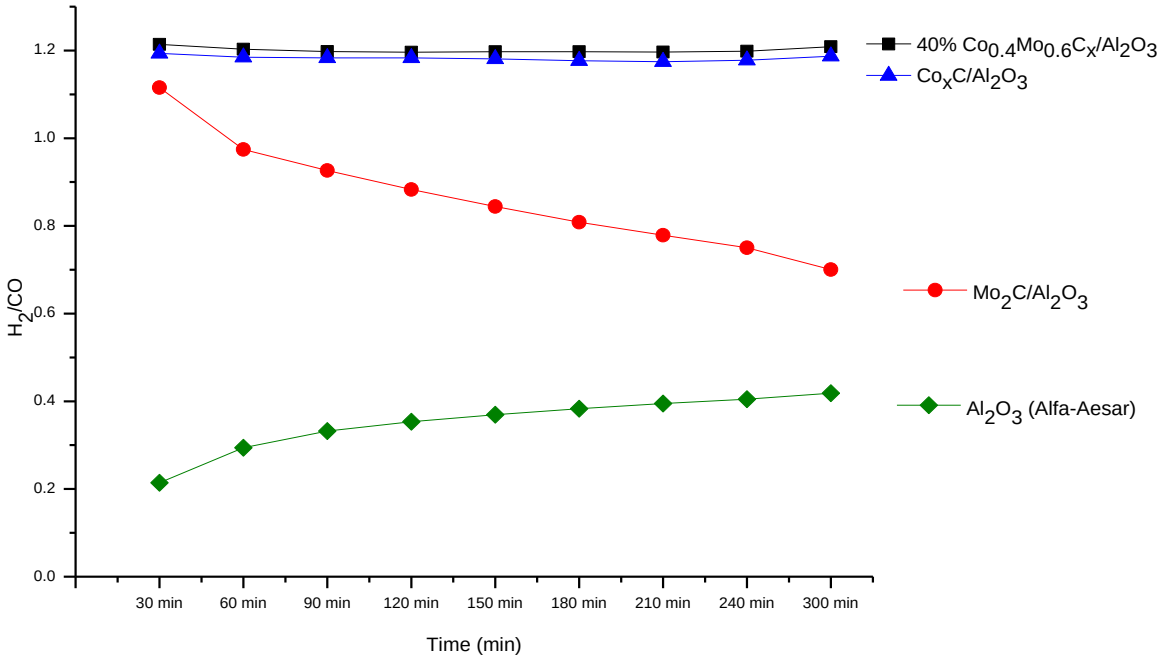


Figure 31: Dependence of the reaction product ratio (H_2/CO) on reactions time for supported carbides at 850°C.

The reaction under study as shown in Figure 31 above is the DMR. It is thought that the reaction produces 2 moles of CO and 2 moles of H_2 from 1 mol of CO_2 and one CH_4 groups as shown in equation 1.5.

It has been evidenced from the literature that the molar ratio of H_2/CO remains practically always below one for the DMR reaction. Studies show that this is due to the side reaction occurring between CO_2 and H_2 as shown below in equation 1.6.

This means that the amount of H_2 formed during the DMR reaction decreases and thus, gives a molar ratio less than 1. It is interesting to note that from our experimental results two catalysts ($Co_{0.4}Mo_{0.6}C_x$ and Co_xC) yield H_2/CO ratios greater than one. We believe that this might be indicating that the side reaction between CO_2 and H_2 might not occur to such a significant extent. However, we consider that further study is needed to confirm this statement.

It is interesting to note that in the presence of CH_4, another reaction could significantly increase the H_2/CO molar ratio as shown in equation 1.5. This reaction has been the main source of investigations for various studies [63, 64].

The aim of our study is to determine both the conversion ratios of CH_4 and CO_2 as evidenced by the data in Figures 29 and 30 above. Additionally, the product ratios of H_2/CO

for four different catalysts are shown in Figure 31 above. For two catalysts (the bimetallic carbide and the Co carbide) we have noted that the conversion ratio for CH_4/CO_2 remains high for the duration of the experiment. Similarly, the molar ratio of H_2/CO remains above the value of one, indicating that other side reactions might be occurring concomitantly. More specifically, the reaction known as Reverse Water Gas Shift (RWGS) sometimes occurs during the DMR reaction as shown in equation 1.4 [65].

Hence, according to the results presented above the effect of the support cannot only make an apparent higher conversion for both CH_4 and CO_2 but might also decrease the extent of the RWGS reaction that is occurring during the DMR process. It is believed that there is also a possibility for methane decomposition reaction (1.9) which produces carbon and hydrogen. This will also increase the H_2/CO ratio.

3.4 X-ray analysis of catalysts pre and post-reactions

The XRD analysis for both the post-reaction and pre-reaction samples was showing identical results in terms of stability under variable temperature conditions. For this reason, it has been decided to only experiment with the post-stability testing materials.

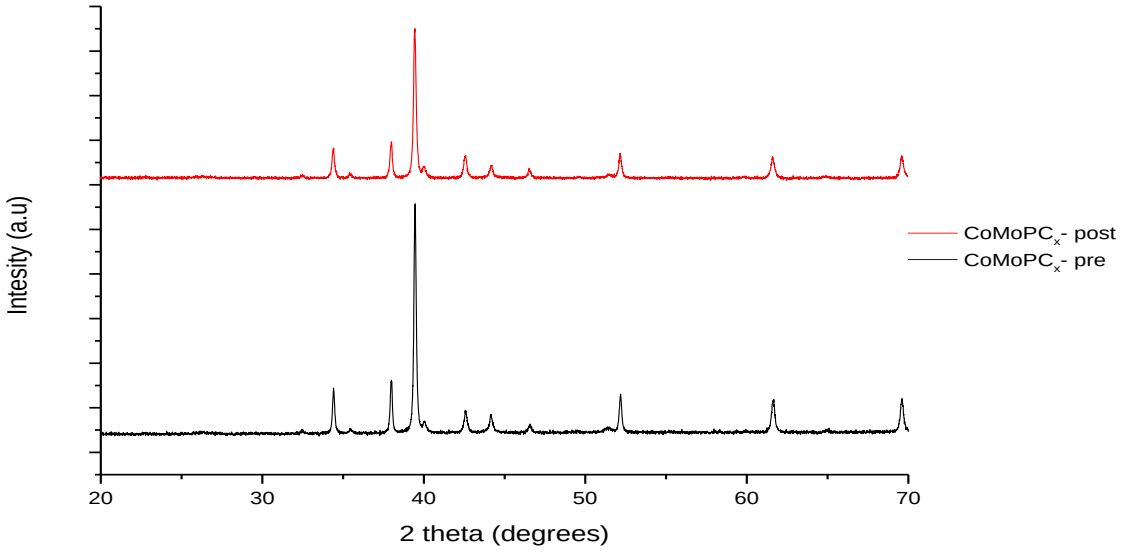


Figure 32: X-ray patterns comparison of $CoMoPC_x$ before and after the catalytic test at 850°C for 300min.

As shown in Figure 32, the results above indicate that the catalyst under study is stable at the conditions that have been previously used since there is no change in the number of peaks of the XRD spectrum between the pre and post-reactions.

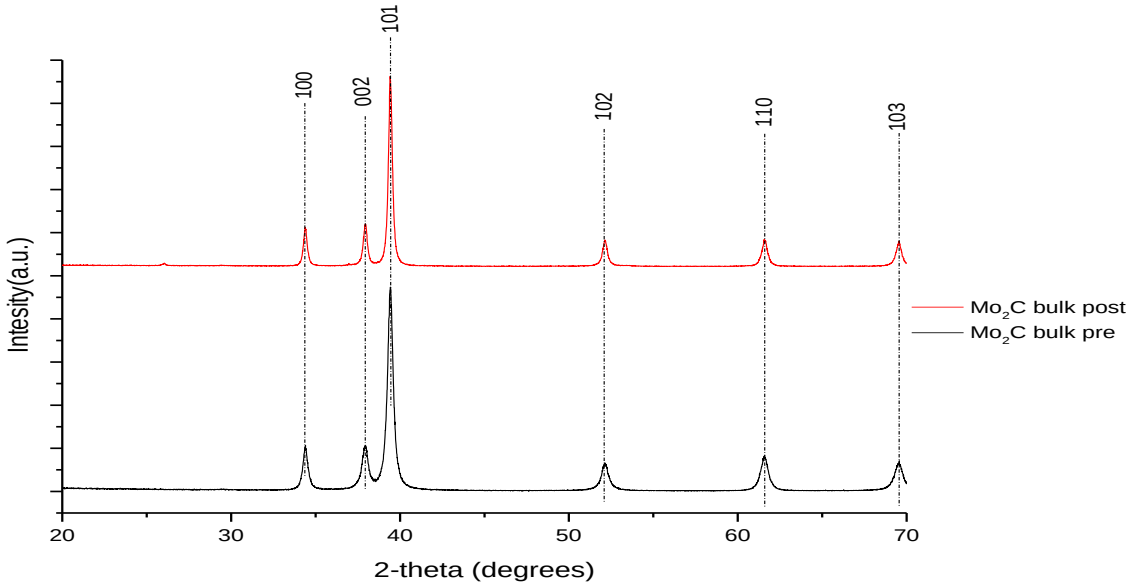


Figure 33: X-ray patterns comparison of both the pre and post-reactions for Mo_2C bulk at 850°C for 300min.

The Mo carbide analysis as shown in Figure 33 above suggests that the catalyst is stable for the range of temperature used for the whole duration of the experiment.

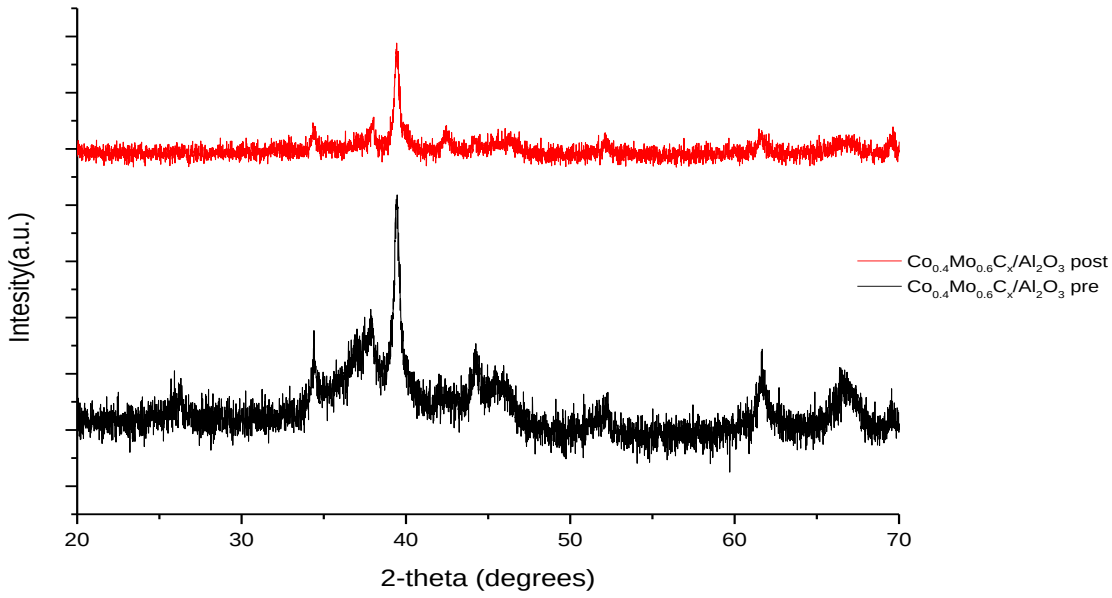


Figure 34: X-ray patterns comparison of both the pre and post-reactions for $Co_{0.4}Mo_{0.6}C_x/Al_2O_3$ at 850°C for 300min.

The difference in peak heights at a 2θ value of around 60-70 degrees as depicted in Figure 34 above may be due to the sensitivity of the XRD experiment. Thus, it is suggested that the pre-run was carried out at a greater sensitivity than the post-run.

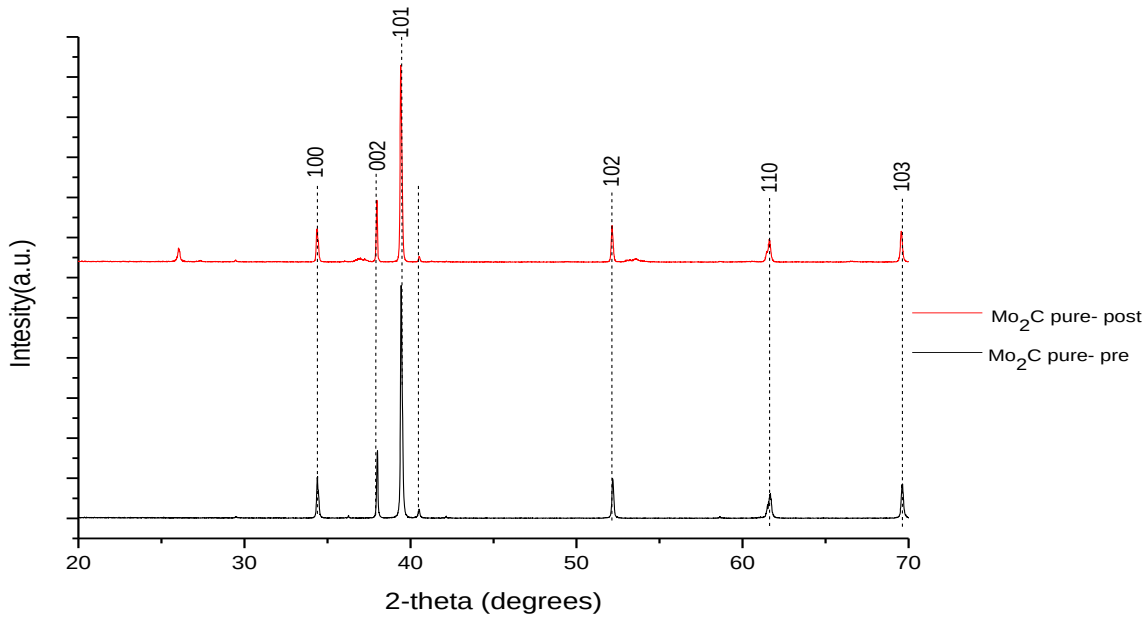


Figure 35: X-ray patterns comparison of both the pre and post-reactions for Mo_2C supplied by Sigma-Adrich at 850°C for 300min.

It seems that some additional peaks appeared during the post-reaction as evidenced in the XRD spectrum (as shown in Figure 35 above). These extra peaks may be attributable to new compounds at the surface or alternatively due to morphological changes that might occur at the surface of the catalyst. However, not sufficient time was allowed to investigate further. Subsequent research is therefore needed to confirm and identify the newly-created products and potential surface changes. Another reason might be that, at some point of the process traces of contaminants have been adsorbed at the surface of the catalyst.

3.5 Discussion

Molybdenum carbide has previously been studied as a catalyst for dry methane forming, with the majority of studies having been carried out over unsupported (bulk) Mo_2C. It has been established that these catalysts possessed reforming activity comparable to noble metals, whilst being noticeably less susceptible to coking than, for example, nickel. For the carbide catalysts, deactivation usually occurred via oxidation of Mo_2C to MoO_2.

In our research, a systematic study of the role of single and mixed metal Mo/Co carbides has been reported, and also catalytic activity investigated for these carbides on a support material.

A summary of our results are presented in Table 2 below. For clarity reasons, the reaction conditions have not been explicitly mentioned and can be found in Chapter 3.

Catalyst	**CH_4 Conversion**	**CO_2 Conversion**	**H_2:CO ratio**
Al_2O_3 support	43% throughout	20% rising to 40% near end	0.2 rising to 0.4
Co carbide bulk	100 %	95%	1 rising to 1.1
Supported Co carbide	100%	>90%	1.2
Mo carbide bulk	Start at 95% then falls to 40%	95% then falls to 50%	1.0 falling to 0.5
Supported Mo carbide 60wt%	Start at 85% then falls to 50%	90% then falls to 60%	1.1 falling to 0.7 near end
Co/Mo carbide bulk	Start at 80% then falls to30%	90 % then falls to 40% followed by slight increase to 60%	0.85 falling to 0.6 near end
Supported Co/Mo carbide	96% throughout	>90% throughout	1.2
$CoMoPC_x$	100% throughout	95% throughout	1.2
Mo_2C (supplied by Sigma-Aldrich)	>10% throughout	Start at 10% rising to 20%	>0.2

Table 2: Summary of the results of the effectiveness of the investigated catalysts on Dry Reforming.

Results for the CH_4 conversion (as evidenced in Figures 20, 23, 26 and 29) indicate that all catalytic materials tested show a rather high activity, even for the Al_2O_3 support. However, for all catalysts, there was a loss in activity of Mo_2C during the testing period.

The CH_4 conversions clearly show differences between the support, bulk Mo_2C and the supported Mo/Co bimetallic carbides. Interestingly, the activity of the Al_2O_3 support in the DMR reaction is significantly higher than the bulk Mo_2C material. The relatively high catalytic activity for the Al_2O_3 support is understandable given the high operating temperatures (> 800 °C) and the high surface area of the support. The lower conversion of CH_4 on bulk Mo_2C may be due to surface area effects, which have limited feedstock adsorption.

The relatively higher activity of supported carbides as compared to the bulk carbide can be understood by rationalising that surface area effects may play an important role in the catalytic activity. A further explanation for the conversion difference between the bulk and supported carbides is the surface effect caused by the Al_2O_3 support, leading to the different dispersion status and different surface area.

CO_2 conversion results (as depicted in Figures 21, 24, 27 and 30) clearly demonstrate that the support exhibits some activity for the reaction under the test conditions, which may be due to the high temperature, which favor the conversion thermodynamically. Additionally, the other three tested materials show appreciable activity. It was also noticed a notable decrease in the catalytic activity of the Mo_2C and in the stability of the other two catalysts. Clearly, the catalytic carbides are considerably more effective in the decomposition of CO_2 than the support alone.

3.5.1 Bulk catalysts (no support)

Results presented in Figures 20-22 and 26-28 show the conversion of CH_4 and CO_2, respectively. The first point to note is that throughout the test the CoC_x shows relatively high conversion of CH_4 and 95% conversion of CO_2. This leads to believe that methane is reacting to potentially form other additional products such as CO and H_2. Since low ratios of H_2/CO would indicate low levels of H_2 and high levels of CO it seems that the RWGS reaction is occurring at noticeable rates on the support itself.

The activity of the mixed Co/Mo carbides (as evidenced in Figures 20-22 and 26-28) for the conversion of CH_4 starts at 80% and falls to 20% after about 90 minutes. CO_2 conversion again starts at around 90% but then falls to 40% after 90 minutes. The molar ratio of H_2/CO is initially 0.85 but falls to about 0.6 indicating that the side reaction RWGS becomes more and more important during the testing.

Interestingly, $CoMoPC_x$ shows extremely high catalytic activity of around 100% throughout the test for both the CH_4 and CO_2 conversions. Similarly, the high H_2/CO ratio indicates that the DMR reaction here is significant and is maintained throughout the duration of the testing.

Co_xC bulk shows similar high activity of 100% for both the CH_4 and CO_2 conversions. The molar ratio of H_2/CO is also maintained near a value of 1 throughout the test indicating that the DMR reaction is occurring.

For the CH_4 conversion the Mo_2C bulk catalyst has an initial high activity of 100% which then falls to 40% and varies from 95% to 50% for the CO_2 conversion. After an initial molar ratio of 1 for H_2/CO this value decreases to 0.5, indicating that the CO production becomes much higher. This may be due to carburisation, which would also explain the loss in activity of the catalyst. However, additional evidence is needed from further investigations.

The results obtained indicate that for unsupported (bulk) catalysts $CoMoPC_x$ and Co_xC show high activity, which is maintained at a temperature of 850°C for the period of the testing. It is also worth noting that both the conversion rates of CH_4 and CO_2 remain quite high.

In contrast, Mo_2C (bulk) shows some activity, which is about half the activity of the other catalysts. However, greater activity has been observed at elevated temperatures indicating that the activity of Mo_2C (bulk) might be temperature-dependent. The greater activity detected at higher temperature could be related to the fact that the reaction under study is endothermic and as such, would be favoured at higher temperatures. Here again, further work is required to investigate these observations.

Both Mo_2C and the mixed carbide ($Co_{0.4}Mo_{0.6}C_x$) show little to no activity (around 3%) compared with the other catalysts under study. These results suggest that the reaction is not only temperature-dependent but it might also mean that significant amount of catalysts are needed before the reaction can actually occur to any significant importance.

3.5.2 Supported catalysts

For the supported mixed Co/Mo carbide both the CH_4 and CO_2 conversions show high rates which are maintained with time and temperature. The H_2/CO ratio of 1.2 indicates that the DMR reaction is continually occurring during the testing period.

For supported Co carbide both CH_4 and CO_2 conversions are high for the duration of the tests, and the H_2/CO ratio of 1.2 is indicating a high production of both H_2 and CO. However, the side reaction RWGS is believed to be becoming prominent which might cause significant deviation.

For supported Mo_2C carbide both the CH_4 and CO_2 conversions start at high levels but then fall to much lower levels; drifting from 85% to 50% for CH_4 and from 90% to 60% for the CO_2 conversion. The molar ratio of H_2/CO also falls from 1.1 to 0.7, indicating a significant decrease of the DMR reaction.

The results presented indicate that both supported bimetallic Co/Mo carbide and Co_xC/γ-Al_2O_3 have high catalytic activity which is then maintained throughout the experiment. This suggests that the catalysts are both stables at temperatures of 850°C.

From our studies it is quite clear that the Al_2O_3 support greatly affects the catalyst activity. This presumably arises from both the varying (enhanced) active catalyst surface area, and the acid-base property of the support itself. Some evidence for the "intrinsic" acid-base catalytic function of the Al_2O_3 support is evident from its very respectable (*ca* 40%) catalytic activity at these high operating temperatures (Table 2). We have not discussed in any detail the precise mechanisms for DMR. However, it is established that CO_2 reforming undoes the adsorption and dissociation of CO_2 on the operating catalysts.

Since CO_2 is of course an acid gas, the adsorption and dissociation of CO_2 will be impaired with a basic catalyst. What is quite clear is that the mixed Mo/Co metal carbides supported on Al_2O_3 are particularly promising systems for methane dry reforming, with both the Co/Mo and $CoMoPC_x$ showing no appreciable sign of deactivation after dry reforming for extended periods at these high operating temperatures.

Chapter Four: Conclusions

4 Conclusions

Dry-methane reforming is an attractive route for potential CO_2 utilisation. It attracts continued interest from industrial and environmental standpoints as it represents the conversion of two greenhouse gases to synthesis-gas, which can serve as an important feedstock for a variety of downstream processes, e.g. methanol synthesis, Fischer-Tropsch synthesis or ammonia synthesis[1].

Reforming with CO_2 is also attractive in that it can be employed in areas where water is scarcely available. Here our aim was to obtain high-performance catalysts with high stability. Traditionally, precious or noble metal catalysts have been used, but these also catalyse coke formation leading to significant deactivation of catalysts. In this work, a series of Co, Mo and Co/Mo bimetallic carbide catalysts have been prepared and their catalytic performance in the methane reforming reaction investigated. We find that the carbides of Mo and Co – particularly these mixed metal carbides – exhibit excellent catalytic activity and most satisfactory stabilities, particularly under these extreme, high-temperature operating conditions. As such they are highly desirable alternatives for noble metal catalysts in these reactions.

Specifically, we have attempted to indentify the best methods and conditions for the formation of the Co/Mo carbides and then their subsequent use as catalysts in various reactions in the methane dry reforming reaction.

XRD analyses (Figures 32-35) have proven useful in following the reactions path and are successful in determining extents of both catalysis synthesis and catalysis testing reactions. The results have indicated that there is good stability of the majority of the catalysts under study; however there is a surface change in Mo_2C which requires further study.

Tests on the catalytic activity of the bimetallic supported carbides and other catalysts under study show that good catalytic performance was achieved. Additionally, many of the catalysts were stable for the duration of the tests.

[1] CO_2-reforming of methane was in fact first proposed by Fischer and Tropsch as a substitute for the steam reforming of methane.

Most noteworthy were the results that all supported catalysts and the Co_xC bulk catalyst as well as $CoMoPC_x$ all show good stability at temperatures up to 850°C. The exception was the Mo_2C catalyst which shows a significant loss in activity. $CoMoPC_x$, the bimetallic carbide and Co_xC show the greatest activity and are stable under the temperature conditions. For Co_xC, it is clear (as shown in Figure 25) that the H_2/CO ratio is significantly higher than 1:1.25 at temperatures lower than 850°C. This might suggest that the RWGS reaction is occurring and it is becoming less significant with time.

Theoretically, the DMR reaction produces H_2 and CO in the molar ratio of 1:1. A ratio of 1 should therefore be achieved for H_2/CO and any deviation from this theoretical figure indicates that side reactions are occurring simultaneously.

If we highlight the highest performance catalyst, $CoMoPC_x$ further investigation is needed to confirm the exact mechanism of action. One line of further enquiry could centre on the possibility that the addition of phosphorous to $Co(NO_3)_2$, $(NH_4)_3MoO_4$, using H_3PO_4 might accelerate the bond-breaking reactions and thus increase the catalytic activity of $CoMoPC_x$ [66].

Another important aspect of our findings centres on the comparison between supported catalysts with bulk catalyst. For the materials investigated here, the former exhibit the highest catalytic performance and this will need to be balanced with the potential of accelerated oxidation (deactivation) of such catalysts on high surface area supports.

This work has set the scene for future studies to examine the precise origins of the high catalytic performance – and high stability – of the supported mixed Mo/Co carbides by advanced spectroscopic techniques, e.g. Fourier-transformed infrared spectroscopy and photoelectron spectroscopy, for example.

References

1. BP Statistical Review of World Energy June **2011**. (http://www.bp.com/sectiongenericarticle800.do?categoryId=9037128&contentId=7068555)
2. Wender, I., *Ann.Rev.Energy*, **1986**, (11), 295-314.
3. Speight, J.G., Handbook of Industrial Hydrocarbon Processes, *Elsevier Inc.* **2011,** 429-466.
4. King, D.A., *Science,* **2004**, (303), 176-177.
5. Yan, S.-R.; Jun, K.-W.; Hong, J.-S.; Choi, M.-J.; Lee, K.-W., *Appl. Catal. A: Gen.* **2000**, (194-195), 63-70.
6. Centi, G.; Perathoner, S., *Catal. Today*, **2009**, (148), 191–205.
7. Ruckenstein, E.; Wang, H. Y., *Appl. Catal. A: Gen.* **2000**, (204), 257–263.
8. Gang, L.; Chengfang, Z.; Yanqing, C.; Zhibin, Z.; Yianhui, N.; Linjun, C.; Fong, Y., *Appl. Catal. A: Gen.* **1997**, (150), 243-252.
9. Levy, R. B.; Boudart, M. *Science,* **1973,** 181 (4099), 547-549.
10. Ayabe, S.; Omoto, H.; Utaka,T.; Kikuchi, R.; Sasaki, K.; Teraoka,Y.; Eguchi,K., *Appl. Catal. A: Gen.* **2003**, (241), 261-269.
11. Fan, M.-S.; Abdullah, A. Z.; Bhatia, S., *ChemCatChem*, **2009**, (1), 192-208.
12. Xiao, T. C.; York, A. P. E.; Al-Megren, H.; Williams, C.V.; Wang, H.-T.; Green, M. L. H.; *J. Catal*. **2001**, (202), 100-109.
13. Al-Megren,H.; Gonzalez-Cortes, S. L.; Xiao, T.; Green, M. L. H., *Appl. Catal. A: Gen.* **2007**, (329), 36-45.
14. Blanchard, P.; Lamonier, C.; Griboval, A.; Payen, E., *Appl. Catal. A: Gen.* **2007**, (322), 33-45.
15. Fang, K.; Li, D.; Lin, M.; Xiang, M.; Wei, W.; Sun, Y., *Catal. Today*, **2009**, (147), 133-138.
16. York, A. P. E.; Xiao, T.; Green, M. L. H., *Top. Catal.* **2003**, (22), 354-358.
17. Jiang, Z.; Xiao, T.; Kuznetsov, V. L.; Edwards, P. P., *Phil. Trans. R. Soc. A.* **2010,** (368), 3343-3364.
18. Trimm, D. L., *Catal. Today*, **1999,** (49), 3-10.

19. Kothari, R.; Buddhi, D.; Sawhney, R. L., *Renew. Sust. Energy Rev,* **2008,** (12), 553-563.
20. Wang, S.; Lu, G. Q. M.; Millar, G. J., *Energ. Fuel*, **1996,** (10), 896-904.
21. Choudhary, T. V.; Choudhary, V. R., *Angew. Chem. Int. Ed.*, **2008,** (47), 1828-1847.
22. Darujati, A. R. S.; Thomson, W. J., *Appl. Catal. A: Gen.* **2005,** (296), 139-147.
23. Levy, R. B.; Boudart, M., *Science,* **1973,** (181), 547-549.
24. Claridge, J. B.; York, A. P. E.; Brungs, A. J.; Marquez-Alvarez, C.; Sloan, J.; Tsang, S. C.; Green, M. L. H., *J. Catal.* **1998,** (180), 85-100.
25. Darujati, A. R. S.; Thomson, W. J., *Chem. Eng. Sci.* **2006,** (61), 4309-4315.
26. Brungs, A. J.; York, A. P. E.; Claridge, J. B.; Marquez-Alvarez, C.; Green, M. L. H., *Catal. Lett.* **2000,** (70), 117-122.
27. Xiao, T.; York, A. P. E.; Coleman, K. S.; Claridge, J. B.; Sloan, J.; Charnock, J.; Green, M. L. H., *J. Mater. Chem.* **2001,** (11), 3094-30998
28. Erdohelyi, A.; Cserenyi, J.; Papp, E.; Solymosi, F., *Appl. Catal. A: Gen.* **1994,** (108), 205-219.
29. Fujishima, A.; Zhang, X., *Comptes Rendus Chimie,* **2006,** (9), 750-760.
30. Ferreira-Aparicio, P.; Rodriguez-Ramos, I.; Anderson, J. A.; Guerrero-Ruiz, A., *Appl. Catal. A: Gen.* **2000,** (202), 183-196.
31. Gallego, G. S.; Batiot-Dupeyrat, C.; Barrault, J.; Mondragon, F., *Ind. Eng. Chem. Res.* **2008,** (47), 9272-9278.
32. Hanaor, D. A. H.; Sorrell, C. C., *J. Mater. Sci.* **2011,** (46), 855-874.
33. Jongsomjit, B.; Wongsalee, T.; Praserthdam, P., *Mater. Chem. Phys.,* **2005,** (92), 572-577.
34. Naito, S.; Tsuji, M.; Miyao, T., *Catal. Today,* **2002,** (77), 161-165.
35. Ledoux, M. J.; Hantzer, S.;Huu, C. P.; Guille, J., Desaneaux, M.-P., *J. Catal.* **1988,** (114), 176-185.
36. Ledoux, M.J.; Pham-Huu, C., *Catal. Today,* **1992,** (15), 263-284.
37. Chorley, R. W.; Lednor, P. W., *Adv. Mater.*, **1991,** (3), 474-485.
38. Leclercq, L.; Provost, M.; Pastor, H.; Grimblot, J.; Hardy, A. M.; Gengembre, L.; Leclercq, G., *J. Catal.* **1989,** (117), 371-383.
39. Zeng, D.; Hampden-Smith, M. J., *Chem. Mater.* **1993,** (5), 681-689.
40. Volpe, L.; Boudart, M., *J. Solid State Chem.* **1985,** (59), 348-356.
41. Wrobleski, J. T.; Boudart, M., *Catal. Today*, **1992,** (15), 349-360.

42. Shi,X.-R.; Wang,S.-G.; Wang,H.; Deng,C.-M.; Qin,Z.; Wang,J., *Surf. Sci.***2009**, (603), 117-122.
43. Page, K.; Li Jun; Savinelli, R.; Szumila, H.N.; Zhang J.; Stalick, J.K.; Proffen, T.; Scott, S.L.; Seshadri, R., *Solid- State Sci.* **2008**, (10), 1499-1510
44. Hilmen, A.-M.; Xu, M.; Gines, M. J. L.; Iglesia, E., *Appl. Catal. A: Gen.* **1998**, (169), 355 - 372.
45. Smith, G. W.; Ibers, J.A., *Acta Cryst*. **1965**, (19), 269.
46. Eda, K.; Uno, Y.; Nagai, N.; Sotani, N.; Whittingham, M. S., *J. Solid State Chem.* **2005**, (178), 2791-2797.
47. Lin, S. S.-Y.; Thomson, W. J.; Hagensen, T. J.; Ha, S. Y., *Appl. Catal. A: Gen.* **2007,** (318), 121-127.
48. Al-Megren, H.; Xiao, T.; Gonzalez-Cortes, S. L.; Al-Khowaiter, S. H.; Green, M. L. H., *J. Mol. Catal. A: Chem*. **2005**, (225), 143-148.
49. Karasek, F.W. and Clement, R., *"Basic Gas Chromatography – Mass Spectrometry"***,** Elsevier, **1988.**
50. Settle F., *"Gas chromatography mass spectrometry"*, Handbook of Instrumental Techniques for Analytical Chemistry, Hites A., Prentice Hall, **1997**.
51. Liu, S. T.; Dong, Q.; Ohnishi, R.; Ichikawa, M., *Chem. Commun.* **1997**, 1455-1456.
52. Lacheen, H .S.; Lglesia, E.; *J. Catal*. **2005**, (230), 173-185.
53. Cheng, J.; Huang, W., *Fuel Process. Technology*, **2010**, (91), 185-193.
54. Wang, J.; Ji, S.; Yang, J.; Zhu, Q.; Li, S., *Catal. Commun*. **2005**, (6), 389-393.
55. Leisegang, T.; Levin, A. A.; Walter, J.; Meyer, D. C., *Cryst. Res. Techno*. **2005**, (40), 95-105.
56. Ding,Y.; Wang,Y.; Su, L.; Bellagamba, M.; Zhang, H.; Lei, Y., *Biosens Bioelectron.* **2010**, (26), 542-548.
57. Bulavchenko, O.A.; Cherepanova, V.S.; Malakhov, V.V.; Dovlitova, L.S.; Ishchenko, A.V.; Tsybulya, S.V., *Kinet. Catal.* **2009,** 50 (2), 205-211.
58. Will, G.; Masciocchi, N.; Parrish, W.; Hart, M., *J. Appl. Chem*. **1987**, (20), 394-401.
59. Korlann, S.; Diaz, B.; Bussell, M. E., *Chem. Mater*. **2002**, (14), 4049-4058.
60. Montesinos-Castellanos A., Lima E., Vázquez-Zavala, A.; de los Reyes, J. A.; Vera, M. A. *Rev. Mex. Ing. Quím.* **2012**, (11), 105-120

61. Euzen, P., Raybaud, P., Krokidis, X., Toulhoat, H., Le Loarer, J.-L., Jolivet, J.-P. and Froidefond, C. *Alumina, in Handbook of Porous Solids,* Edited by F. Schuth, **2008**, 1591-1677, Wiley-VCH Verlag GmbH
62. Montesmos-Castellanos, A., Zepeda, T. A., Pawelec, B., Lima, E., Fierro, J. L. G., Olivas, A. and de los Reyes-Heredia J.A.. *Appl. Catal. A: Gen.* **2008**, (334), 330-338.
63. US patent number 6773691 B2. Controlling syngas H_2/CO ratio by controlling feed hydrocarbon composition.
64. Treacy, D.; Ross, J.R.H., *Prepr. Pap. Am. Chem. Soc., Div. Fuel Chem*. **2004**, 49 (1), 126-127.
65. Choi, S.; Kim S.; Han, C.; Yoon, E.S., 18th European Symposium on Computer Aided Process Engineering. Braunschweig B. and Joulia X . (Editors) **2008** Elsevier B.V./Ltd.
66. Sundaramurthy V., Dalai A.K., Adjaye J., *Catal. Today,* **2007**, 125 (3-4), 239-247